5-2005

Assessments of Vibratory Handheld Tools and Handle Interactions

Douglas Alan Logsdon
University of Tennessee - Knoxville

To the Graduate Council:

I am submitting herewith a thesis written by Douglas Alan Logsdon entitled "Assessments of Vibratory Handheld Tools and Handle Interactions." I have examined the final electronic copy of this thesis for form and content and recommend that it be accepted in partial fulfillment of the requirements for the degree of Master of Science, with a major in Engineering Science.

Jack F. Wasserman, Major Professor

We have read this thesis and recommend its acceptance:

Richard J. Jendrucko, Arnold Lumsdaine

Accepted for the Council:
Carolyn R. Hodges

Vice Provost and Dean of the Graduate School

(Original signatures are on file with official student records.)

To the Graduate Council:

I am submitting herewith a thesis written by Douglas Alan Logsdon entitled "Assessments of Vibratory Handheld Tools and Handle Interactions." I have examined the final electronic copy of this thesis for form and content and recommended that it be accepted in partial fulfillment of the requirements for the degree of Master of Science, with a major in Engineering Science.

Jack F. Wasserman
Major Professor

We have read this thesis
and recommend its acceptance:

Richard J. Jendrucko

Arnold Lumsdaine

Accepted for the Council:

Anne Mayhew
Vice Chancellor and
Dean of Graduate Studies

(Original signatures are on file with official student records.)

ASSESSMENTS OF VIBRATORY HANDHELD TOOLS AND HANDLE INTERACTIONS

A Thesis Presented for the

Master of Science Degree

The University of Tennessee, Knoxville

Douglas Alan Logsdon

May 2005

DEDICATION

This thesis is dedicated to my parents, Mr. and Mrs. Tim and Eileen Logsdon, my sister, Dr. Cheryl Logsdon Knight, and my close friends, Katie L. Padgett, Thomas E. Grass, and Erik G. Hamm, for their encouragement and support throughout my academic career.

ACKNOWLEDGMENTS

This thesis was made possible through the support and guidance of many people. Firstly, I would like to thank Dr. Jack F. Wasserman for giving me the great opportunity of working with him. His knowledge and expertise in the field of Human Body Vibration proved to be invaluable. I would also like to that Mr. Donald Wasserman, who aided me both personally and professionally, and whose contribution to the field of Occupational Safety is without equal. Lastly I would like to thank my committee members for their assistance.

I would also like to thank Ms. Katie Lin Padgett, who provided much needed support and encouragement, as well as contributing to the final editing of this document.

ABSTRACT

There has been a broad history of injuries occurring as the result of vibratory hand-tool use. Following these findings, three human safety standards have been proposed. These standards declare that the dynamic properties with respect to acceleration frequency spectra must be determined for vibratory hand tools. These properties must meet specific tolerances in order to be considered acceptable for use.

The standards, however, do not recognize the significance of the coupling characteristics and the energy transfer between the user and vibrating handle. This interaction reveals the amount of vibratory energy that enters the user's hands. Epidemiological data for VWF shows that certain zones of the hand are first affected causing the onset of disease. Hence vibration is most severe at specific locations on the hand.

The aim of this study was to measure the coupling forces on the hand during the operation of several tool types in real-world working conditions. Simultaneous measurements of force and acceleration were examined in order to determine similarities and differences of the resulting frequency spectra. Transfer functions were used to validate these relationships although non-linearity of the hand system may reduce the values of coherence. In addition, force variations at the finger and palm with respect to coupling dynamics and hand geometry were assessed. Finally, the reliability of the resistive-based force instrumentation system used in this study to produce accurate and repeatable measurements was assessed.

TABLE OF CONTENTS

LIST OF TABLES

LIST OF FIGURES

NOMENCLATURE

m/s^2	meters per second squared
Hz	hertz
lbs	pounds
SCFM	standard cubic foot per meter

Abbreviations

CTS	carpal tunnel syndrome
DAT	digital audio tape
DC	direct current
HAVS	hand-arm vibrations syndrome
VWF	vibration white finger

Symbols

$a_{h,w}$	weighted acceleration
K	weighting factor
rms	root mean squared
t_i	exposure time
T	total test time

1.0 INTRODUCTION TO VIBRATING HAND-HELD TOOLS

Dr. Maurice Raynaud first noted in 1862 a condition where the fingers became white and cold as a result of exposure to cold (13). It has been well documented that individuals utilizing vibrating tools on a regular basis may develop symptoms identical to those observed by Raynaud. This irreversible condition, characterized by finger blanching and permanent vascular damage, has been referred to as Vibration Induced White Finger (VWF), Raynaud's Phenomenon of Occupational Origin, and collectively as Hand-arm Vibration Syndrome (HAVS).

In 1983, the National Institute for Occupational Safety and Health (NIOSH) released a bulletin verifying the prevalence of the disease in the workplace thus declaring its seriousness. Recommendations to better identify and reduce worker's exposure to vibratory hand tools were released in order to educate and protect those at risk (10).

To assess the damaging effects of tool use, several standards have been written. Standards have been developed by the International Organization for Standardization, the American National Standards Institute, and the American Conference of Governmental Industrial Hygienists. The standards set limits on the acceleration magnitudes that a tool can produce in order to be considered safe. Measurements of the transfer of energy from the tool to the user have not been established in these standards.

HAVS affects approximately 5 to 8% of the population. Females contribute to about 90% of these diagnosed cases (13). Within particular industries, the prevalence of the disease may be particularly high.

As yet, there are no methods to treat HAVS. The presence of the disease is not apparent until vibration syndrome is fully developed at which point the condition cannot be reversed. In an attempt to suppress the growing size of the afflicted community, several standards have been written from documented cases as a risk assessment for an individual's potential to develop the syndrome. Though the etiology of HAVS is not well understood, further studies have been conducted in order to better understand the physiological mechanism responsible for the syndrome.

Vibration energy is transmitted via coupling of the operator's hand(s) with the handle of the vibrating tool. The vibration characteristics of the tools vary with respect to vibration magnitude and frequency as well as dominant vibration axes. Variables such as grip force, feed force, hand-tool contact surface area, and posture are factors that contribute to the transmission of the energy. Latency, the duration between first exposure to vibration and the development of symptoms, and prevalence, the number of cases in a population of hand-held tool operators, are important parameters whose characteristics are determined by the preceding variables.

Three vibratory tool types, impact, axial and transverse rotary, will be tested in this analysis. The three tool types represent a sample of various tool types frequently used in industry. The dynamic force and acceleration frequency spectrums will be compared to determine their representation of the vibratory fingerprint of the tool. In addition, the force and acceleration spectrums for each tool will be compared between tool types to reveal the differences in the dynamic tool-operator coupling. Finally, dynamic data will be collected to examine the coupling characteristics at different locations on the tool handle.

2.0 BACKGROUND

A typical hand-arm vibration analysis begins with the assessment of the risks involved with the probability of a tool operator developing symptoms of vibration syndrome which includes blanching of the finger tips as a result of changes in vascular tone. Though the physiological basis of the syndrome is not well known, it is believed that the mechanism by which blanching occurs is the result of an exaggerated central sympathetic reflex that is responsible for the vasoconstrictive response. Three standards have been developed to assess the severity of a vibratory tool. Each standard sets forth guidelines by which equipment, methods, and analysis techniques are well defined. Following a 3rd octave analysis, the data is superimposed on a defined curve set represent limits correlating to a statistical representation of vibration exposure required to cause vibration syndrome. These vibration limits are defined by their corresponding standards. The standards do not assess measurements of the coupling interaction between the tool and its operator with respect to vibration exposure. Such information may be obtained through static and dynamic force measurements as well as handle ergonomic studies.

2.1 SYMPTOMS OF VIBRATION SYNDROME

The development of Vibration White Finger is contributed to by vibration duration and magnitude as well as other factors including tool type and condition, tool operation method, temperature and humidity changes, and alcohol and drug use. Tool

operation factors include the magnitude and direction of the feed force, ergonomics and hand positioning, and hand-tool coupling.

Attacks of VWF are often triggered by cold but can occur as a result of any changes in vascular tone (8). Biological effects of hand-transmitted vibration exposure may include neurological, peripheral vascular, muscular, skeletal, and central nervous system disorders. Initial symptoms include numbness of the fingers. Blanching of the fingertips is typically observed as the dominant symptom at later times of exposure. As the disease progresses, attacks become more severe and more frequent. Taylor and Pelmear have quantified the developmental stages of VWF (see Table 2.1). New scales, such as the Stockholm Workshop scale, have been suggested as a revision to the Taylor-Pelmear scale. This scale disregards tingling and numbness as a symptom of vibration syndrome because it cannot be tested objectively and is susceptible to patient suggestion. Both classification systems are accepted for medical diagnoses.

Once developed, there are no cures for Vibration White Finger. Medical treatments are limited to drugs and therapy. Vasodilators are frequently administered to

Table 2.1: Taylor-Pelmear System for VWF Classification (11)

Stage	Condition of Digits
0	No symptoms
0_T	Intermittent tingling
0_N	Intermittent numbness
1	Blanching of one or more fingertips
2	Blanching beyond one or more fingertips
3	Extensive blanching of fingers with frequent episodes
4	Extensive blanching of most fingers with frequent episodes

patients to offset the narrowing of the peripheral vessels. Other attempts have been made to dilate the peripheral vessels via chemotherapy, a procedure with a high potential of health risks.

2.2 Physiological Basis for Vibration Syndrome

The pathology of VWF is not well understood, but several mechanisms have been hypothesized. It has been observed that exposure to vibration may cause changes in peripheral circulation, finger temperature, and changes in blood pH and viscosity. Vibration exposure initiates an exaggerated vasocontrictive response that compromises blood flow through the digital arteries (8).

Bovenzi et al. observed excessive sympathetic outflow contributing to digital vasoconstriction (3). These changes induced both a reduction in blood flow and skin temperature. Vascoconstrictive responses were recorded in both the vibrated and non-vibrated fingers of subjects. This observation suggests that a central sympathetic reflex mechanism is operative following exposure to vibration. Prolonged exposure to vibration may lead to permanent changes in digital vasculature leading to symptoms associated with vibration syndrome (2).

Futatsuka et al. have observed similar occurrences during chain saw operation. Finger blood pressure appears to be a direct measure of the extent of the vasconstrictive response (7). In addition, it was suggested that the grasping force may dictate the extent of the localization of sympathetic effects.

Re-gripping of the handle of a vibrating tool may be responsible for shocks transmitted to joints causing wrist damage (12). Schenk emphasized that the gripping forces of the vibrating tool be considered as well as the dose-effect relationship in order to successfully prevent bone and joint damages.

2.3 DEVELOPMENT OF STANDARDS

Several standards have been developed from the etiological data and history of VWF. These standards are not based on the actual mechanism of VWF episodes, but rather statistically significant occurrences. The standards recognize that long-term vibration exposure may lead to the development of vibration disease. Guidelines are presented for the recording and measurement of hand-held tools as well as equipment requirements, methods, and analysis techniques. Such guidelines are imposed in order to determine the potential risk of developing vibration syndrome in the workplace. Several standards have been put into practice. All standards analyze a vibration situation by measuring the acceleration values of three principle axes in m/s^2 or g's (*where* 1g = 9.81 m/s^2) at the location of hand/tool coupling via accelerometers. The principle directions are defined by the orthogonal basicentric or biodynamic coordinate system (see Figure 2.1). This data is then processed and weighted according to the standards and the vibration situation is compared to defined vibration thresholds.

ISO 5349-2-2000 assesses a vibration situation based on the total time of vibration exposure (typically 4 hours of an eight hour workday). This exposure is

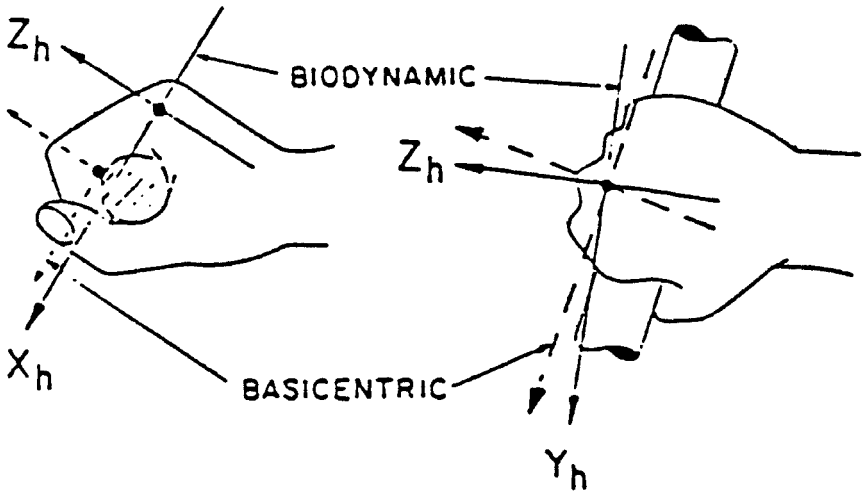

Figure 2.1: Orthogonal Basicentric or Biodynamic Coordinate System (ISO 5349 and ANSI S3.34-1986)

represented as an energy equivalent (rms) acceleration and can be calculated for any length data series:

$$(a_{h,w})_{eq(T)} = \left\{ \frac{1}{T} \sum_{i=1}^{n} \left[(a_{h,w})_{eq(t_i)} \right]^2 t_i \right\}^{1/2}$$
$$T = \sum_{i=1}^{n} t_i \qquad (2.1)$$

where $(a_{h,w})_{eq}$ is the weighted rms acceleration and t_i is the total time of acceleration of the i^{th} operation period contributing to the total test time, T (if testing is not continuous) Equation 2.1 represents the average, or equivalent, acceleration during testing. The rms accelerations are to be reported independently:

$$a_{eq} = \left(\frac{T_1}{T} a_1^2 + \frac{T_2}{T} a_2^2 + \ldots + \frac{T_n}{T} a_n^2 \right)^{1/2} \qquad (2.2)$$

where T_n corresponds to the amount of time of exposure to the acceleration a_n contributing to the total time, T. Acceleration values are weighted according to octave bins from 6.3-1250 Hz using equation 2.3:

$$a_{h,w} = \sqrt{\sum_{j=1}^{n} (K_j a_{h,j})^2} \tag{2.3}$$

where $a_{h,j}$ is the rms-acceleration of 3rd-octave bin j and K_j is the weighting factor.

ISO 8662-1 through 8662-14 implement standards to be applied to specific tool types. Standards for the recording and measurement of hand-held tools are presented. In addition, equipment requirements, methods, and analysis techniques are stated.

Another standard, ACGIH-TLV, follows the previous standard's analysis. Acceleration magnitudes are determined along the ordinate axes of the basicentric coordinate system. The vibration exposure is presented as a single equivalent acceleration value (see Equation 2.1). Additional criteria for the assessment of the severity of vibration exposure are suggested as threshold limits. The Threshold Limit Values (TLV's) are presented in Table 2.2 for various exposure times. Exposure durations greater than 8 hours correspond to a small limit for maximum magnitudes of acceleration are not recognized by the standard.

The "Guide for the Measurement and Evaluation of Human Exposure to Vibration Transmitted to the Hand" is presented in ANSI S3.34-1986. Hand-transmitted vibration exposures are evaluated based on the frequency spectrum of vibration, rms acceleration, direction of transmitted vibration, duration of exposure (1/day) and total time, as well as

Table 2.2: Threshold Limit Values for Various Exposure Times in the X, Y, and Z Directions (ACGIH-TLV 1984-1998)

Total Daily Exposure Duration	Maximum Dominant, Frequency-Weighted Acceleration $(a_{h,w})_{eq}$	
	m/s^2	g^{Δ}
4 hours and less than 8	4	0.40
2 hours and less than 4	6	0.61
1 hour and less than 2	8	0.81
less than 1 hour	12	1.22

Δ: $g = 9.81\ m/s^2$

temporal exposure. Additional criteria for safe working environments have been represented as limits for vibration exposure (see Figure 2.2). These limits correlate to the time of exposure required for development of vibration syndrome as observed by Taylor and Pelmear. Once determined, the processed data may be superimposed on the limit curves in order to assess the potential risk of developing vibration syndrome for a specific vibration scenario. Dong et al. have reported results that suggest that the frequency weightings used by these current standards underestimate vibration risks when measurements are recorded at the finger-tips as well as underestimating the response of the hand-arm system (4, 5).

It is suggested that a dose-effect relationship be determined for the total duration of vibration exposure. As the time of continuous vibration exposure increases, the rms-acceleration may not be representative of the severity of the vibration exposure. Infrequent, high-acceleration magnitudes (impacts) become less significant to the rms calculation as the duration of exposure increases. A fourth-power time dependency

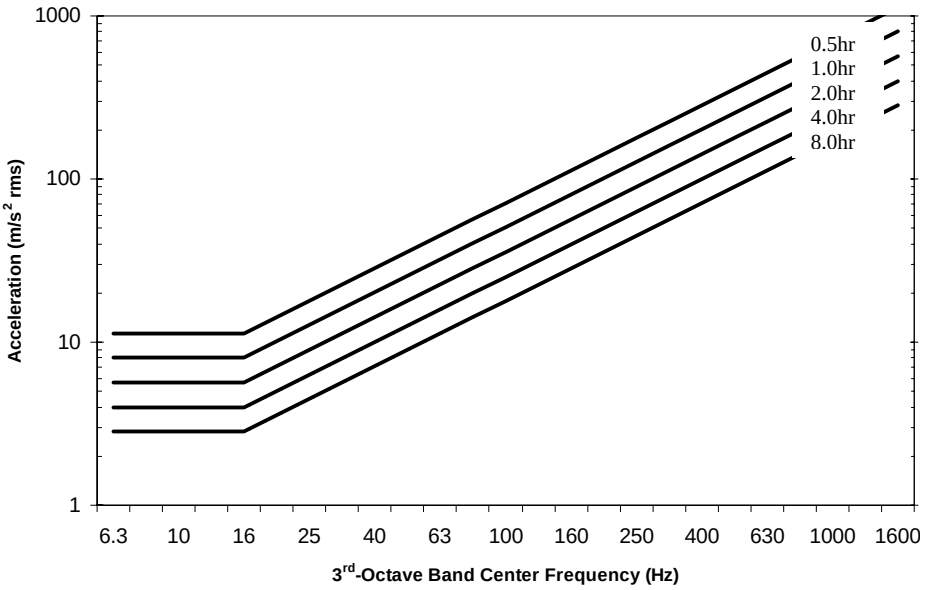

Figure 2.2: Vibration Exposure Curves (ANSI S3.34-1986)

(i.e. Vibration Dose Value or VDV) may be appropriate to account for exposures to impact during long ranges of vibration exposure (8):

$$VDV = \left[\frac{T_s}{N} \sum_{i=1}^{N} x^4(i) \right]^{1/4} \tag{2.4}$$

where T_s is the duration of vibration exposure, and x(i) is the i^{th} exposure magnitude.

2.4 GLOVE TRANSMISSIBILITY

Another standard was developed to evaluate the effectiveness of gloves. ISO 10819:1996(E) is the first standard that assesses vibration transmission from a tool to the user through gloves. The standard sets forth a measurement scheme in which acceleration is measured at a reference point, the handle interface, as well as on the hand.

The impending vibration is experimentally produced such that it is representative of actual working place conditions. Measurement trials are conducted on both a gloved and bare hand. Glove transmissibility, the mean of the ratios of transmissibility between hand and handle for gloved and bare hands, must meet the following criteria for medium and high-range frequency spectra:

$$TR_M < 1.0 \qquad TR_H < 0.6 \qquad (2.5)$$

The glove transmissibility is evaluated at the palm of the hand but not at the fingers. Hence the overall protection of the hand from the glove is not established. In addition, the impending vibration is artificially produced and not be representative of actual vibration experienced during tool use. Also, this system is not able to evaluate the effectiveness of the gloves against impacts, or forces applied at 0 Hz.

2.5 VIBRATION CONTROL VERSUS ERGONOMICS

Wieslander et al. have reported that there is a connection between the repetitive hand movements associated with the operation of vibratory handheld tools and the incidence of Carpal Tunnel Syndrome (CTS) (16). Furthermore, the high-force motions of the tools may be significant contributory factors to hazardous wrist trauma and the onset of CTS. Ergonomically designed tool handles provide to a user a comfortable, natural hand position with minimized wrist angles. However, it is possible that such handles may be able to transfer energy even more efficiently from the tool to the hand, contributing to the damage of nerves and thus the physiological pathway of HAVS.

Therefore, particular attention should be devoted to both vibration control and attenuation as well as ergonomic tool design (15).

2.6.0 INSTRUMENTATION: CAPACITIVE VERSUS RESISTIVE FORCE MEASUREMENT SYSTEMS

Two force measurement systems are currently being used to measure the coupling interaction at the hand/handle interface of vibrating tools. The capacitive and resistive systems each have inherent electronic characteristics which contribute to its strength and weaknesses during experimental use. In addition, the dynamic performance of the instruments determine the range over which the two systems produce accurate and significant measurement data. The system must be able to:

- Measure dynamic coupling forces
- Not inhibit normal tool use
- Produce reliable and repeatable measurements

2.6.1 CAPACITIVE FORCE MEASUREMENT SYSTEMS

Capacitive sensors are composed of two metal armatures separated by a dielectric material. The dielectric material is a poor conductor of electricity, but an efficient supporter of electronic fields. As the oppositely charged plates move relative to one another, the capacitance changes in inverse proportion to the separation of the plates. In addition, the capacitance is a function of the area of the plates. It is possible that the change in capacitance during load application may not be a good representation of

applied force when used on tools with small curvature radii as a result of the transducer not being flush with the handle surface. Feutry et al. have reported that a developed capacitive measurement system using NOVEL sensors pressure sensors demonstrated 15% error over a dynamic frequency range from 0-200 Hz (6).

2.6.2 Resistive Finger Force Instrumentation System

The instrumentation system consists of a finger pressure sensor and preamplifier located at the hand and a post-amplification controller (see Figure 2.3). The detector's electrical impedance changes proportionally with force applied to the detector's 10mm diameter surface. The preamplifier then converts this charge into a corresponding electrical voltage of low impedance which is sent to the post-amplification controller unit. Once at the controller, the unit provides additional variable amplification as well as low pass filtering of the signal.

Figure 2.3: DC Electronic Finger Pressure Instrumentation System – Pressure Sensor and Preamplifier

The force instrumentation used in this study was custom designed and built by our University of Tennessee Knoxville group. Analyses have shown that the system is capable of producing reliable and accurate results from 0 to 1600 Hz; capable of measuring both DC as well as frequency dependent components of dynamic forces. The small size of the sensor satisfies dimensional requirements by not disrupting the user's grip on the operating tool, and the supporting electronics have been shown to minimize electromagnetic interference providing that the electronic components of the system are sufficiently shielded. Technical details about the system are published elsewhere (1, 14). It was an objective of this study to verify the repeatability of measurements for this system.

3.0 PROCEDURE

Experimentation was conducted in two stages. In the first stage, three pneumatic tools with unique vibration characteristics were tested. Their mechanical attributes represented tools of axial rotary, transverse rotary, and impact type. The latter stage of testing was conducted with the intent of identifying the significance of the placement of the finger sensor. Pressure measurements were recorded on both the finger and palm sides of the handle of a reciprocating saw. Finally, consecutive tests were performed using this tool in order to evaluate the force system's ability to produce repeatable measurements. Simultaneous measurements of finger pressure and tri-axial acceleration were recorded for all experiments in accordance with current hand-arm standards. The experimental set-up is shown in Figure 3.1. Data for all tool tests where recorded for 1.5 minutes.

3.1 PRESSURE SENSOR LOAD APPLICATION/CALIBRATION

Load was applied to the force sensor through a load application apparatus (see Figure 3.2). The load force was applied in one pound increments, up to 10 pounds, via a c-clamp and the output voltage was recorded from the force sensor's main amplifier. Tests were conducted on a single channel at full-gain. In order to determine pressure distribution effects on the sensor's output voltage, three load application scenarios were devised: (1) load applicator is steel with a contact area equal to the sensor's area, (2) the load applicator is steel and the contact area is less than that of the sensor's area, and (3)

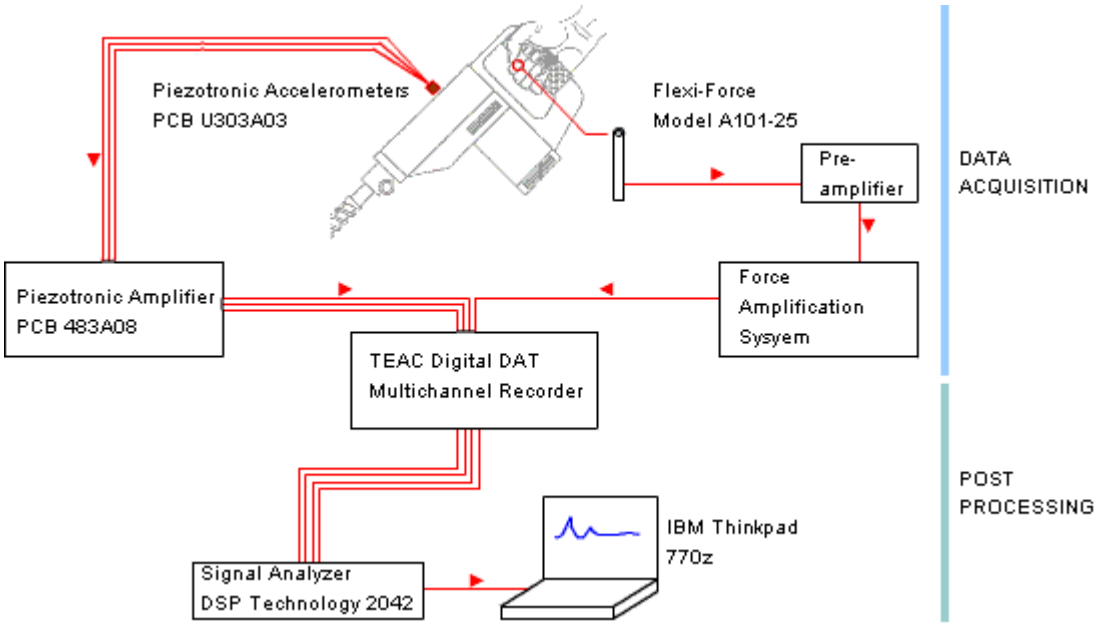

Figure 3.1: Experimental Set-Up for Simultaneous Force and Acceleration Measurements. Arrows indicate signal direction.

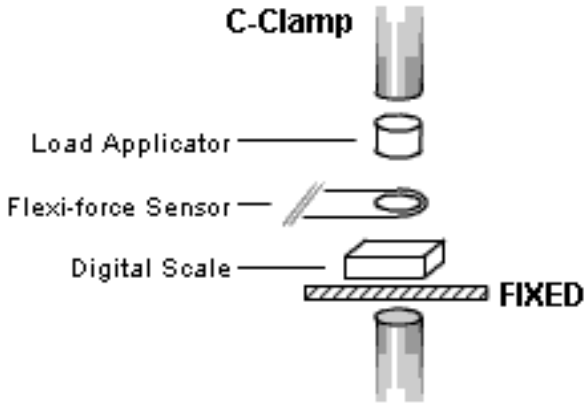

Figure 3.2: Set-Up for Determining Pressure Distribution Effects on the Force Instrumentation System's Output

the load is applied through a visco-elastic material exhibiting material properties identical to that of anti-vibration gloves available in industry.

3.2 IMPACT TOOL TEST

A pneumatic impact hammer was instrumented with a tri-axial accelerometer set-up in accordance with the Basicentric Coordinate System (see Figure 3.3.a). To induce potential variations in working conditions, splitter and flat chisel bits were used. The pressure sensor was secured directly to the index finger at the middle phalanx. The tool operated at 28 SCFM (standard cubic foot per minute) regulated at 90 psi at 3500 strokes per minute. A realistic working environment was simulated by removing a 1" thick layer of plaster from a 14" masonry block's surface (see Figure 3.3.b). All data was recorded on a DAT recorder for post processing.

Figure 3.3: (a) Impact Hammer Instrumented with Tri-axial Accelerometer and Fitted with Flat Chisel and Splitter Bits and (b) Impact Hammer In Use

3.3 DRILL TOOL TEST

A pneumatic drill was fitted with a 3/8" masonry bit and instrumented with a tri-axial accelerometer set-up in accordance with the Basicentric Coordinate System (see Figure 3.4.a). The pressure sensor film was placed over the middle phalanx of the index finger and was securely fastened. The drill operated at 10 SCFM at a regulated pressure of 90 psi. The tool speed was approximately 500 rpm. In order to duplicate the tool working environment, holes were drilled into a concrete block (see Figure 3.4.b).

3.4 GRINDER TOOL TEST

The tri-axial accelerometer set-up was mounted onto a pneumatic grinding tool in accordance with the Basicentric Coordinate System (see Figure 3.5.a). The pressure sensor film was placed over the middle phalanx of the index finger and was securely fastened. Operation of the tool was at 6 SCFM regulated at 90 psi. At this pressure, the tool speed was approximately 25000 rpm. The working environment was replicated by grinding a 2" L-bracket (see Figure 3.5.b).

Figure 3.4: (a) Pneumatic Drill with 3/8" Masonry Bit and (b) Drill In Use

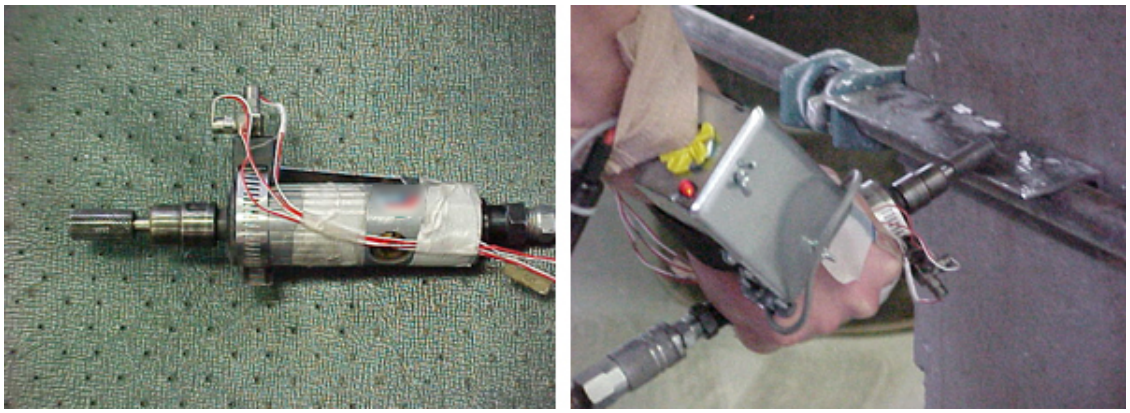

Figure 3.5: (a) Instrumented Pneumatic Grinder and (b) Grinder In Use

3.5.0 RECIPROCATING SAW TOOL TESTS

An electric reciprocating saw was used to evaluate the force instrumentation system. The effects of pressure sensor placement as well as the systems ability to reproduce measurements were evaluated. For each case, the saw was instrumented with a tri-axial accelerometer set-up in accordance with the Basicentric Coordinate System. The pressure sensor was mounted directly to the primary grip of the saw's handle (see Figure 3.6). The saw was equipped with an 18 tpi (tooth per inch) bi-metal cutting blade and was operated at a setting that produced maximum vibrations for this particular saw (setting 4-of-6). The saw was used to cut through a ¼" thick steel plate. The cutting blade was replaced for the reproducibility measurements because of the dulling of the blade for the previous test measurements.

3.5.1 PRESSURE SENSOR PLACEMENT

Two tests were employed in order to quantify the significance of the placement of the sensor. First, the sensor was fastened to the front of the grip directly behind the

Figure 3.6: Reciprocating Saw Instrumented with Finger Pressure Sensor

middle phalanx of the middle phalange. For the final test, the sensor was attached to the rear of the grip handle so that it was in direct contact with the bony phalange joint of the thumb. The two locations where selected such that the sensor was in contact with hard tissue of the hand.

3.5.2 REPEATABILITY

Three tests where performed with the saw measuring acceleration and force at the palm side of the handle. Each test was performed ten minutes apart. A static measurement of force was made before and after each dynamic test was conducted. For the static tests, a mass was placed on the sensor through a load applicator which matched

the surface area of the force sensor. The combined weight of the mass and load applicator was 2.27 lbs and was selected such that a sufficient change in voltage was produced by the sensor. The tests were performed to document reproducibility of measurements.

4.0 RESULTS & DISCUSSION

After the data was collected, frequency analyses were performed. Data was sampled at 0.625 Hz and 20 samples were averaged. The frequency spectra for force and the dominant vibration axis were compared to determine similarities between the two types of measurements. Transfer functions, or output/input relationships, were calculated for the acceleration and force data in order to identify zones where measurement similarities exist. Each respective coherence function was then calculated to determine the confidence in the transfer functions. Coherence functions combine the relationships of magnitude and phase angle to validate that these output/input relationships are consistent and independent of magnitude. A value of 1 means the compared signals are completely consistent. When the value is 0, the output is caused by sources independent of the input. Hence, the coherence function is a measure of the validity of the estimated transfer function. Analyses conducted in accordance with the current hand-arm standard are included in Appendix D. Violations of the standard occur when the limits proposed by the standard have been exceeded.

4.1 IMPACT HAMMER RESULTS

The impact hammer equipped with the chisel bit produced violent motions at the handle during normal tool operation. In addition, the tool exhibited impact characteristics. Dominant peaks within the force spectrum can be seen at several frequencies up to 600 Hz as shown in Figure 4.1. As shown, these peaks are similar to

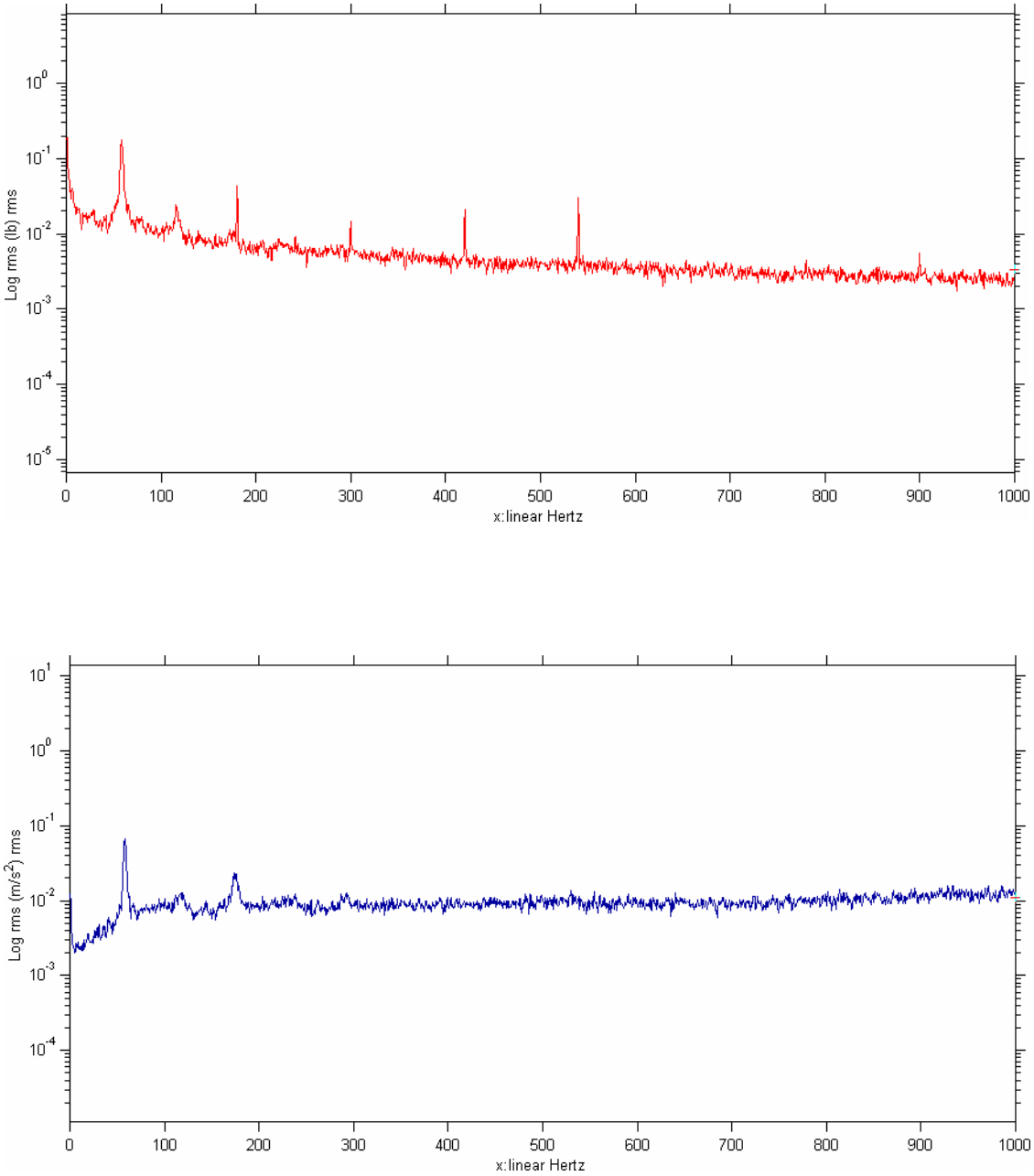

Figure 4.1: Force and Acceleration Frequency Spectrums from Continuous Operation of Impact Hammer with Chisel Tip

the dominant peaks in the z-axis acceleration data for frequencies up to 200 Hz. In addition, attenuations of force magnitudes were observed towards higher frequencies within the entire bandwidth which did not occur in the acceleration spectrum. X and y-axis acceleration data is included in Appendix A.

The transfer function analysis reinforces that there is a relationship between force and acceleration. The first three dominant peaks are consistent between the two measurement types and produce a moderately consistent transfer function within this frequency range (<200 Hz) (see Figure 4.2). However, only the first peak at approximately 50 Hz provided good coherence. Poor coherence at the higher frequencies may suggest possible system non-linearity and/or other phenomena. Additional data for this tool equipped with a splitter bit is included in Appendix B.

4.2 Drill Tool Results

Drill operation consisted of creating multiple holes in a cement block. As shown in Figure 4.3, similarities exist between peaks in both acceleration and force frequency spectra at low frequencies (<100 Hz). The tool produces harmonic peaks in the force frequency spectrum that are not present in the acceleration data throughout the frequency bandwidth. X and y-axis acceleration data is included in Appendix A.

The transfer function reveals an area of consistence between the two measurement systems within the low frequency range (see Figure 4.4). However, the coherence is extremely low within this range indicating the estimated response may not be accurate. Hence, the low frequency similarities between the frequency spectra may not be causal.

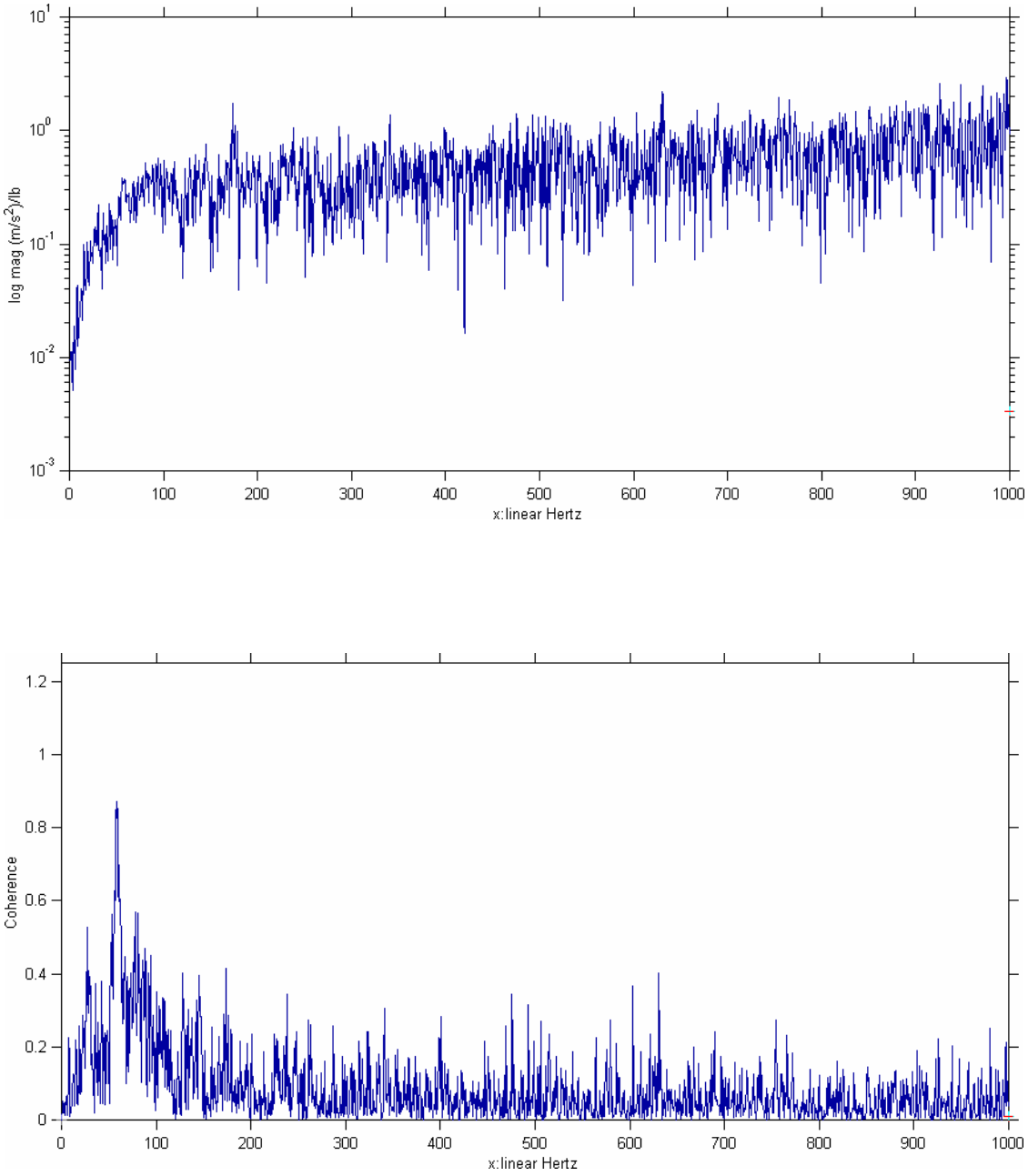

Figure 4.2: Transfer Function and Coherence from Continuous Operation of Impact Hammer with Chisel Tip

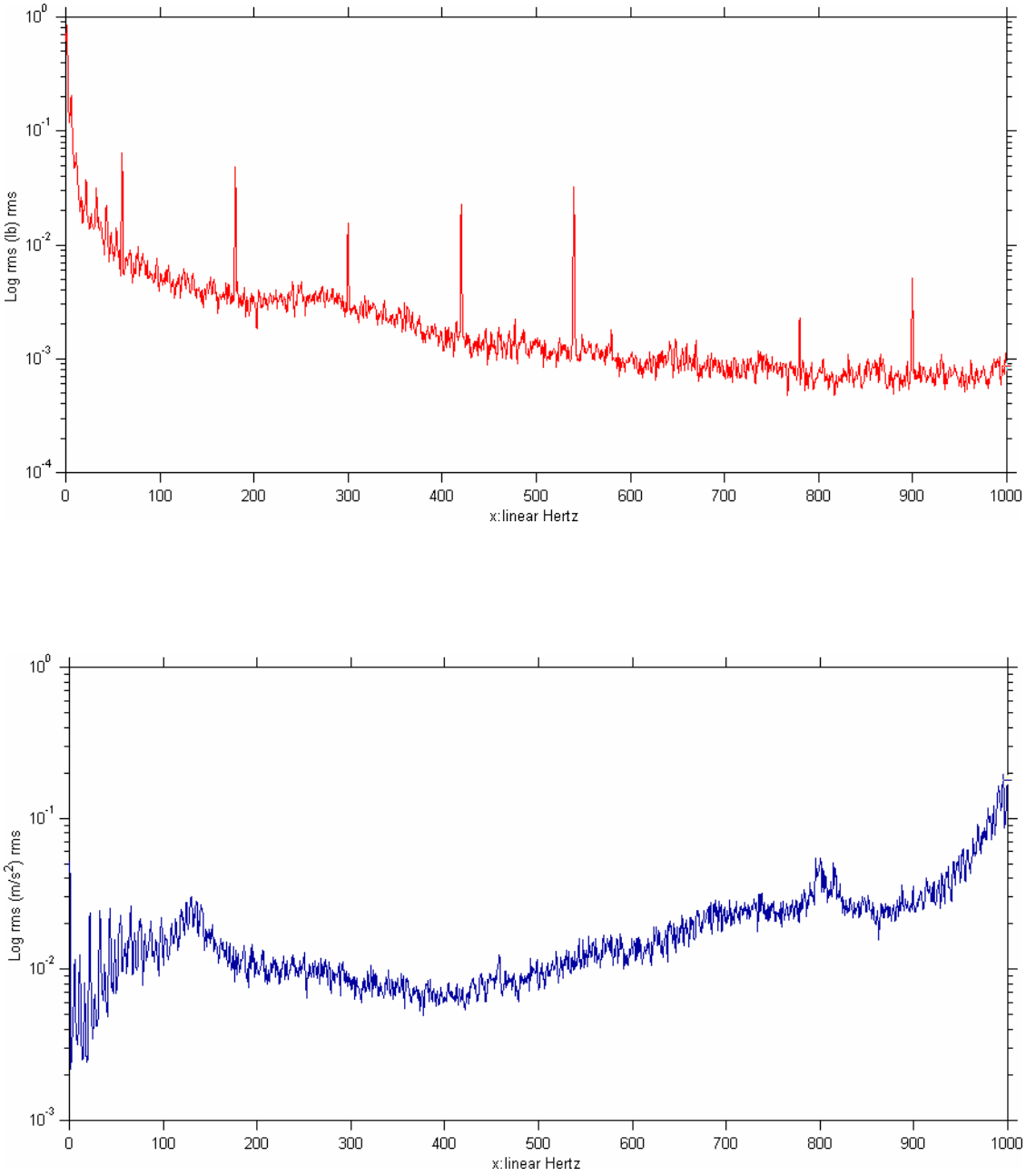

Figure 4.3: Force and Acceleration Frequency Spectrums from Continuous Operation of Drill

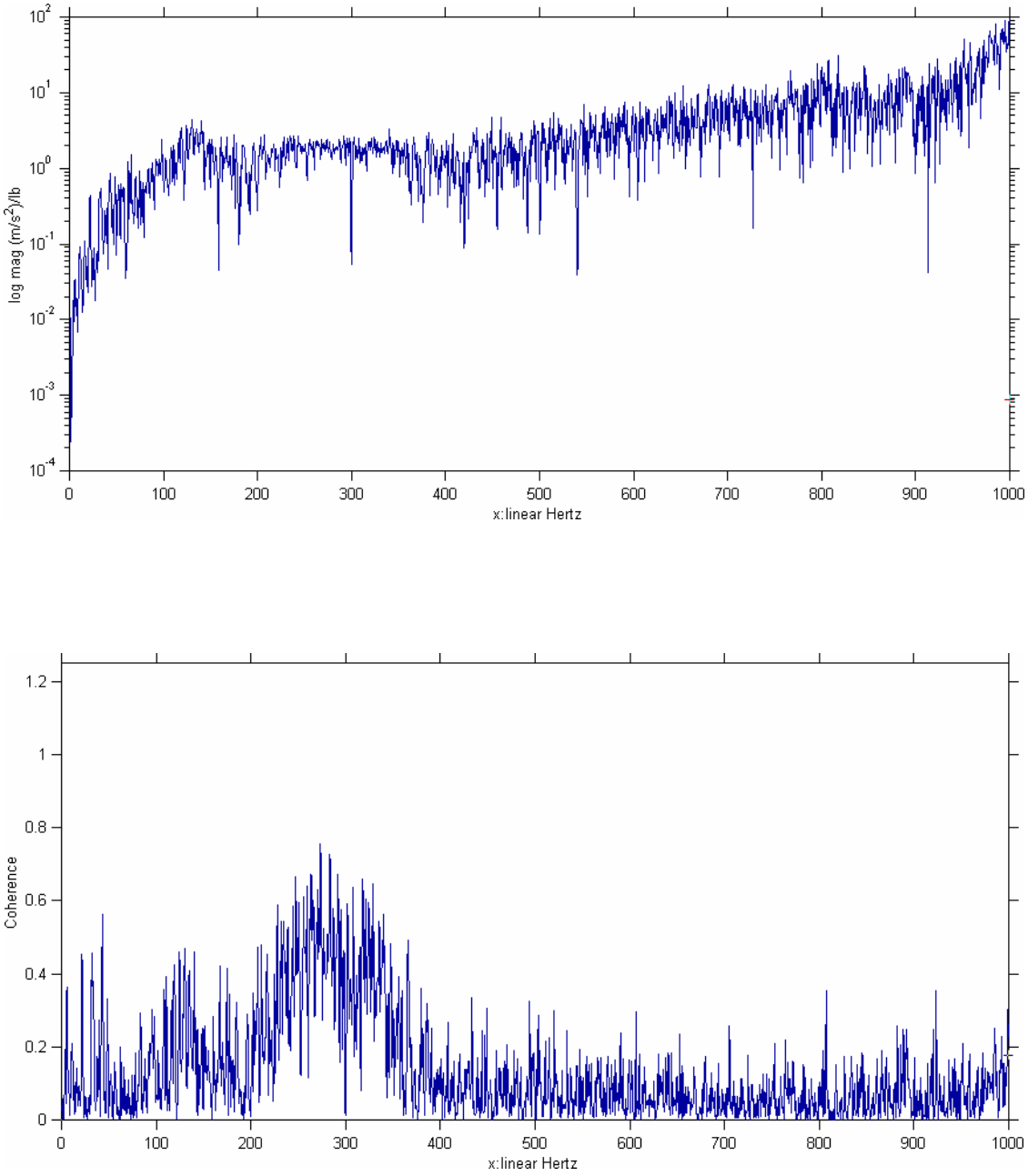

Figure 4.4: Transfer Function and Coherence from Continuous Operation of Drill

4.3 GRINDER RESULTS

As shown in Figure 4.5, there are similarities in the spectra for force and acceleration data through 600 Hz. The magnitudes of both force and acceleration were much lower in magnitude than the drill or the chipper. Again, harmonic peaks can be seen on the force frequency spectrum which are not represented in the acceleration frequency spectrum. Hence, this characteristic can be attributed to the coupling interaction of the user with the tool. The resonant spikes for this tool were much more pronounced than the previous tool types. The spikes may be the result of movement of the force sensor itself. This tool required less grip force to operate than the other tool types. As a result, the coupling of the hand with the tool was less significant. This may allow the force sensor to move with the tissue of the finger, and would be indicative of the tissue response to vibration rather than the coupling of the users hand with the tool handle. Attenuation of the force magnitude was observed at higher frequencies. X and y-axis acceleration data is included in Appendix A.

The transfer function is presented in Figure 4.6. Some consistent zones were observed at frequencies less than 200 Hz, and especially around 100 Hz. These regions exhibited low coherence.

4.4.0 RECIPROCATING SAW RESULTS

As a result of the replacement of a dull cutting blade, some variations in the frequency spectra for force and acceleration were observed between the pressure sensor placement tests and the repeatability tests. However, simultaneous force and acceleration

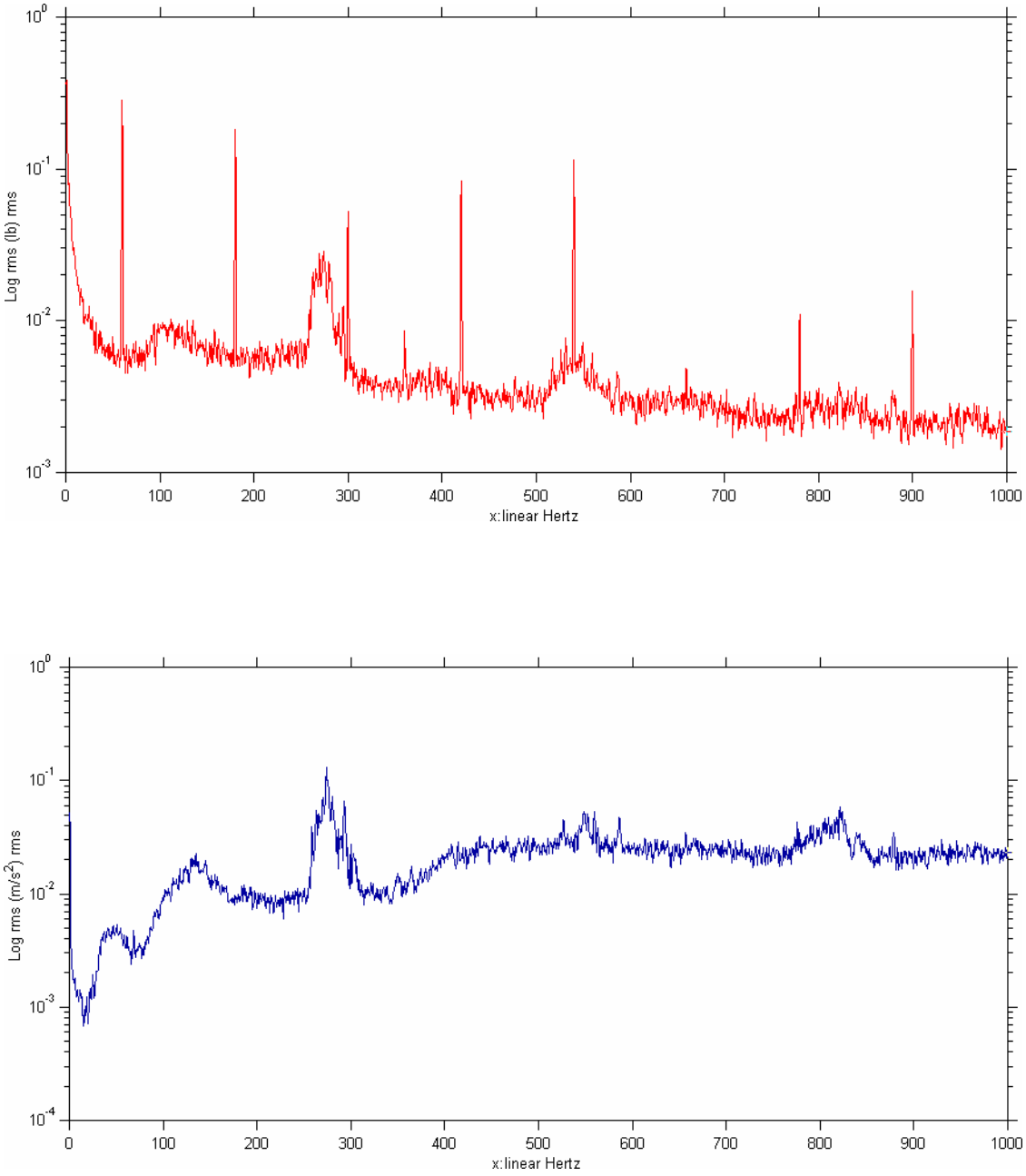

Figure 4.5: Force and Acceleration Frequency Spectrums from Continuous Operation of Die Grinder

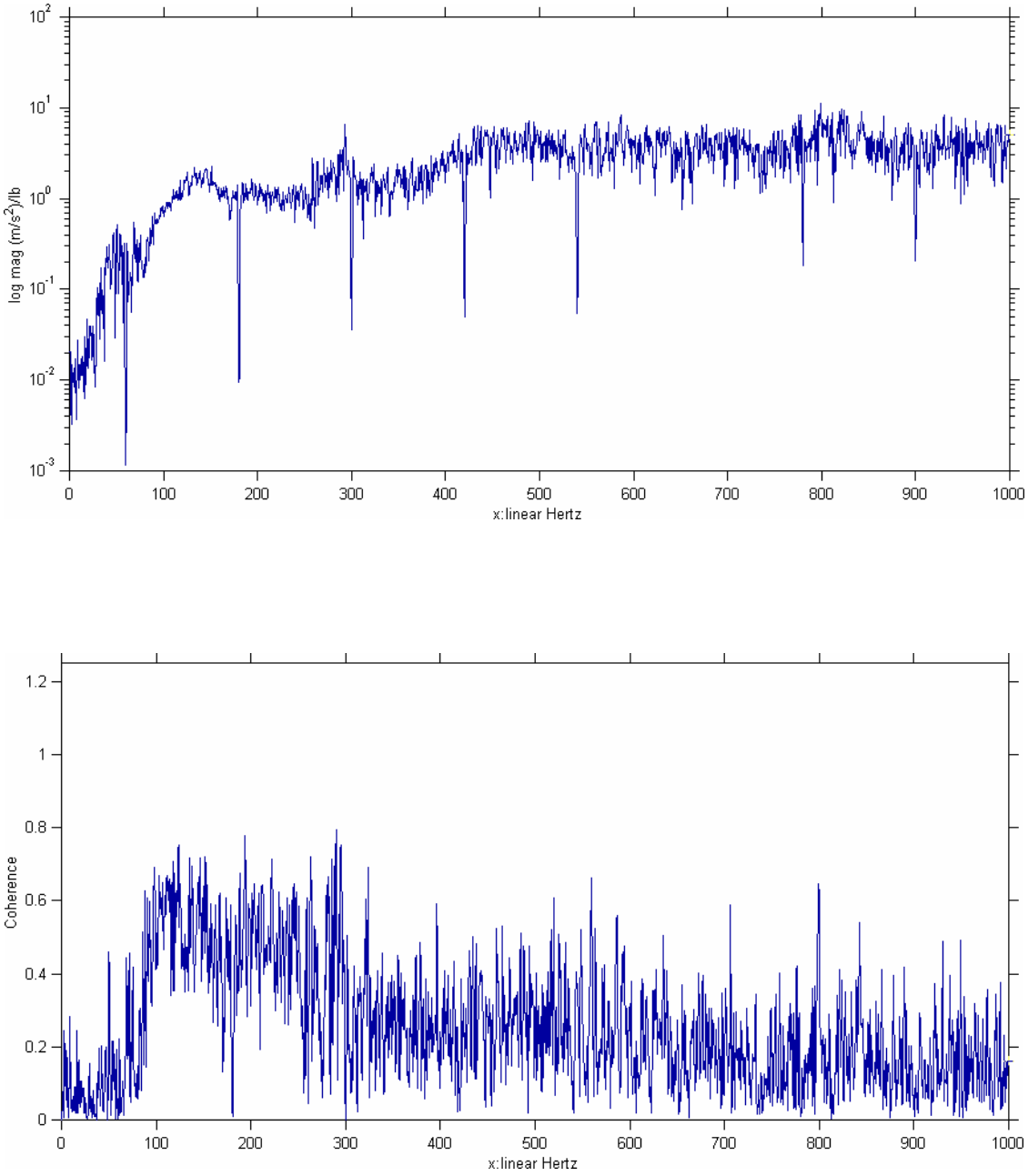

Figure 4.6: Transfer Function and Coherence from Continuous Operation of Die Grinder

measurements within each test remained similar. Hence, the differences can be attributed to the replaced saw blade. Acceleration frequency spectra for the pressure sensor placement test are included in Appendix A. Appendix C contains acceleration frequency spectra from the repeatability tests.

4.4.1 Pressure Sensor Placement

The reciprocating saw produced harmonic peaks that were measured both on the finger and palm of the hand during tool operation (see Figure 4.7). Measurements at both the finger and palm exhibit resonance throughout the frequency bandwidth. Resonant peaks are similar in frequency and dissimilar in magnitude. The dominant peaks for the palm measurements were significantly higher in magnitude. Frequency attenuation was observed throughout the bandwidth for both measurement locations.

With respect to the dominant axis of acceleration, linear frequency responses were observed for frequencies up to 200 Hz (see Figure 4.8 and 4.9). The respective coherence functions reinforce this observation. Though coherence was high for both locations, the consistency of the transfer functions was slightly greater when measurements were made on the bony protuberance of the thumb rather than on the finger.

4.4.2 Repeatability

Static tests revealed that the sensor performed within an average of 25.7% error. Pre and post-trial results for each of the static tests are included in Table 4.1. The force

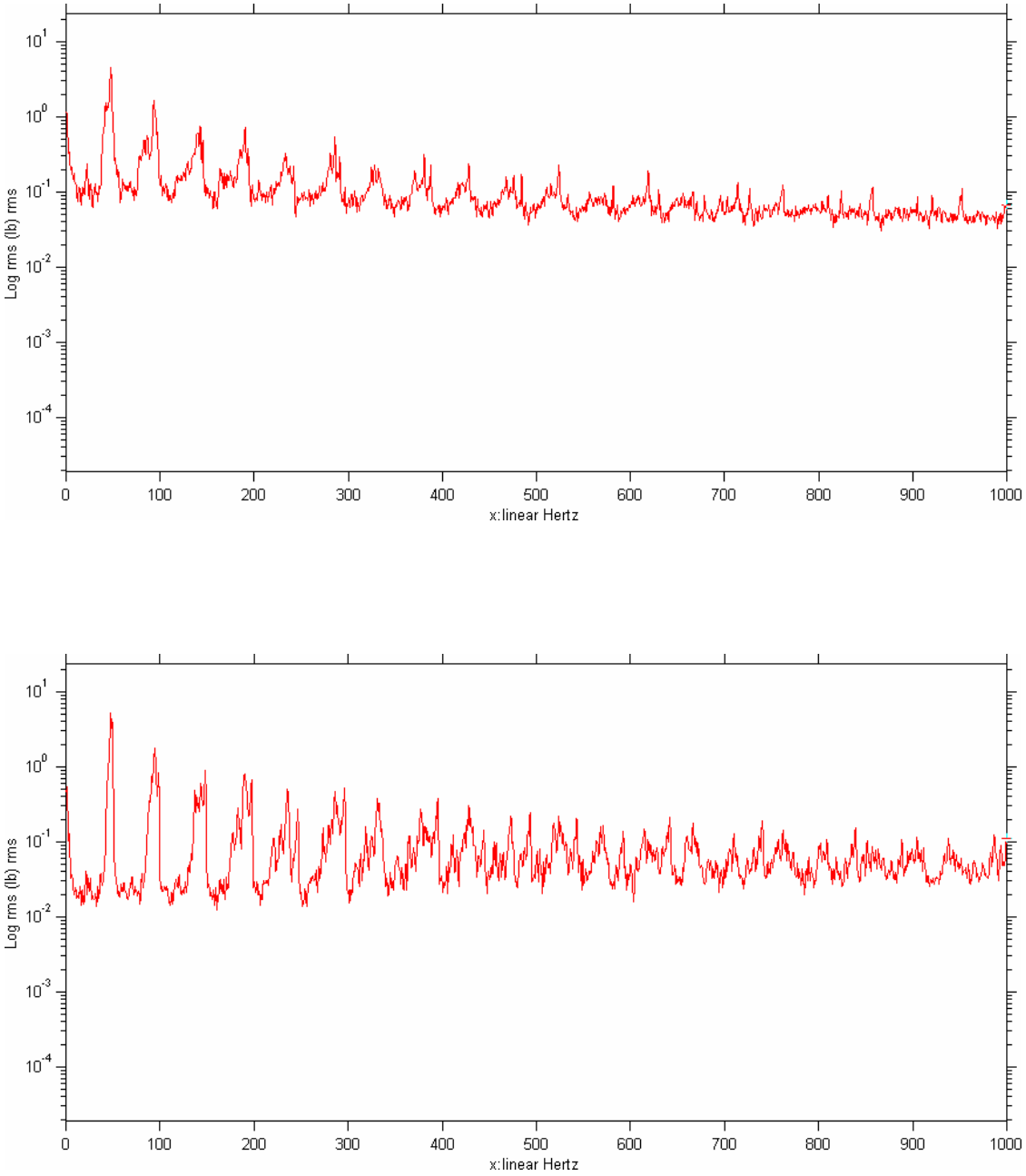

Figure 4.7: Frequency Spectrum Measured from the Finger and Palm of the Hand during Continuous Operation of a Reciprocating Saw

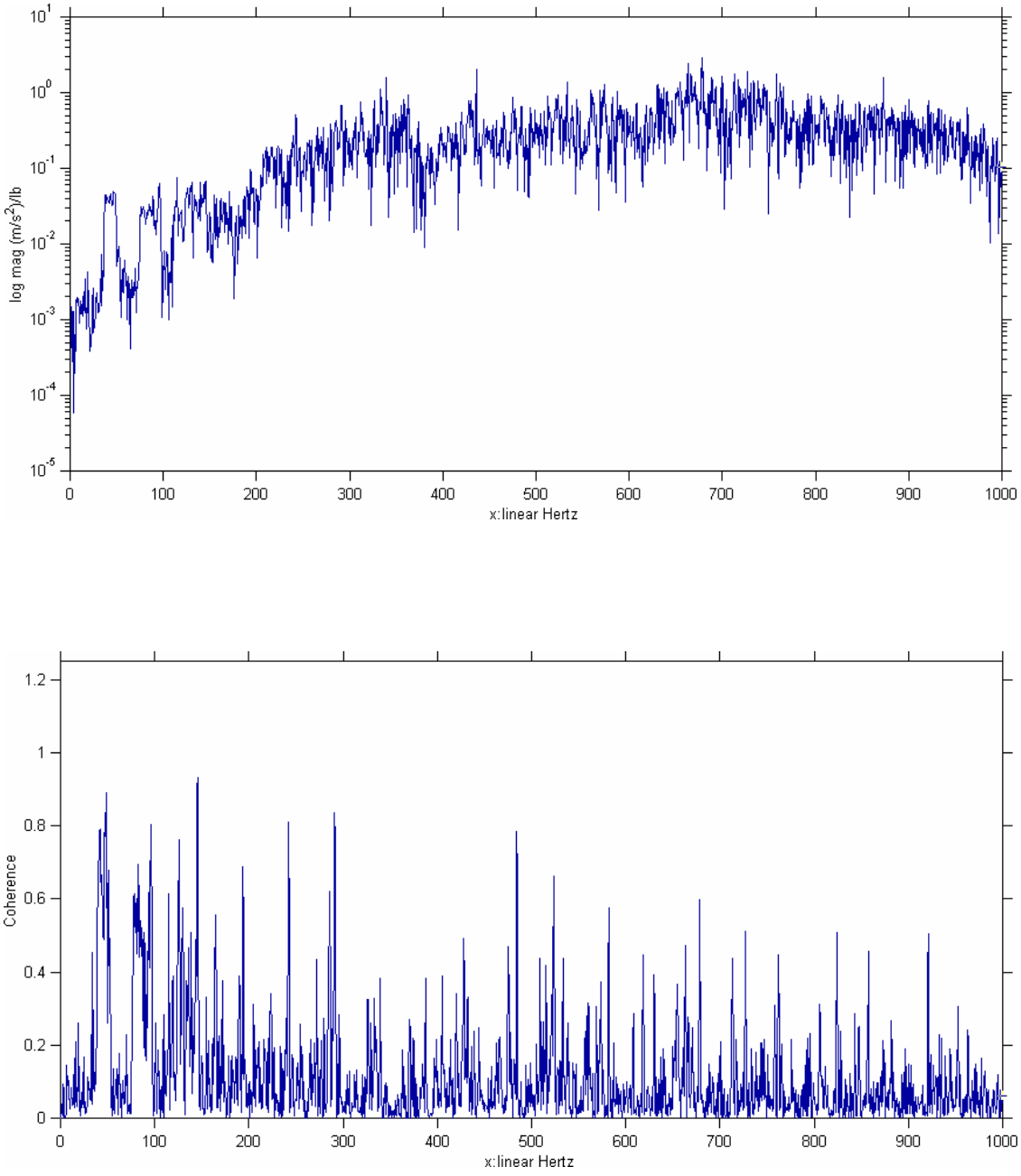

Figure 4.8: Transfer Function and Coherence for Finger Measurement during Continuous Operation of a Reciprocating Saw

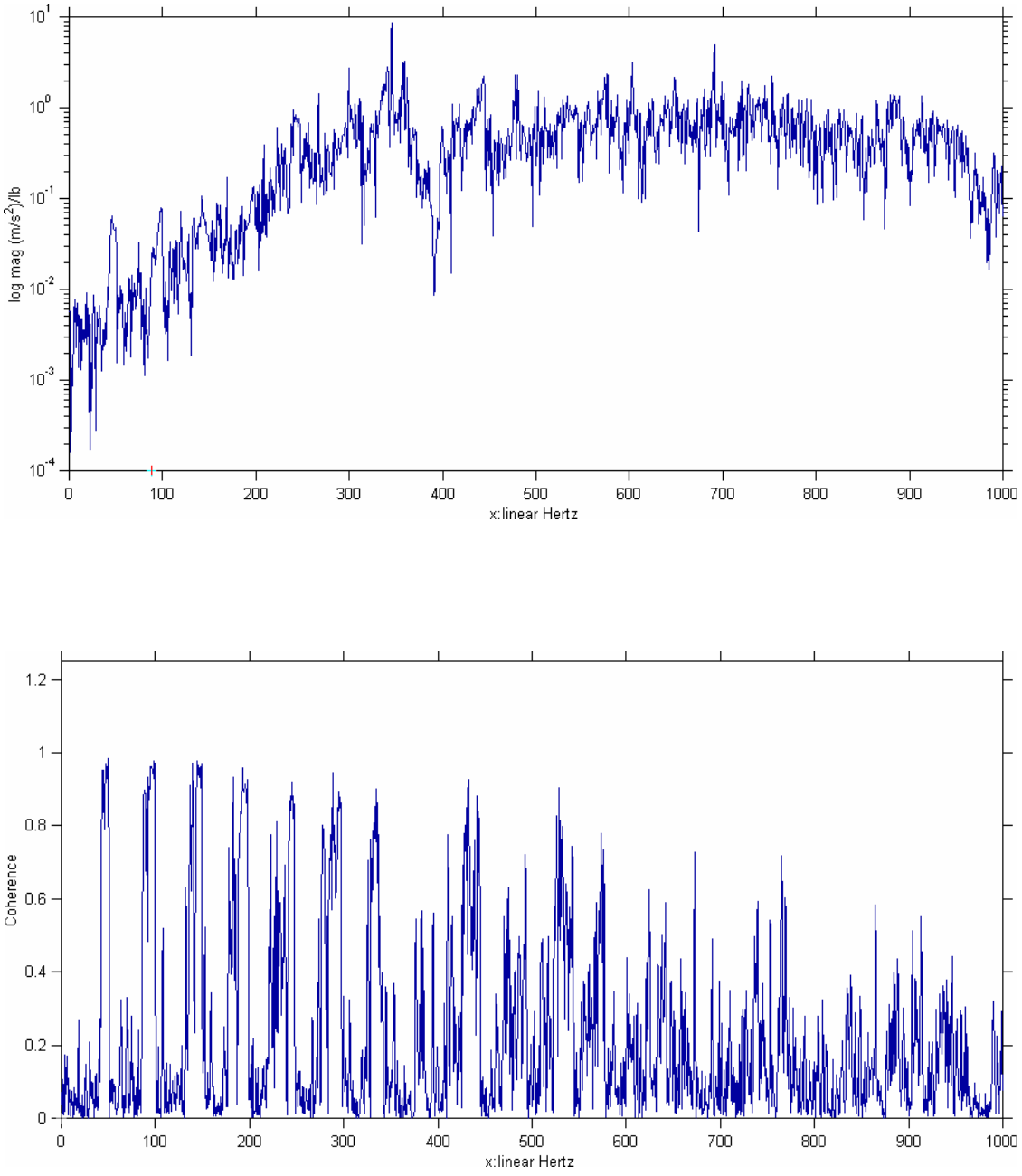

Figure 4.9: Transfer Function and Coherence for Palm Measurement during Continuous Operation of a Reciprocating Saw

Table 4.1: Results from Static Testing of the Force Transducer for Sequential Testing

Trial	Output Voltage (mV)		Error
	pre-Trial	post-Trial	(%)
One	248	128	48.4
Two	268	260	4.76
Three	152	128	23.8

2.27 lbs applied weight for each trial

sensor proved to be accurate in the reproduction of data with respect to frequency. The transducer produced nearly identical frequency spectra throughout the analyzed bandwidth (see Figure 4.10). The force spectra for the three orthogonal axes are included in Appendix C. A reduction in output voltage of the sensor was observed after each measurement trial. Attenuations of voltage may have been the result of the compression of the ink disk. The resistance of the sensor to compression may diminish between tests, thus decreasing the output voltage.

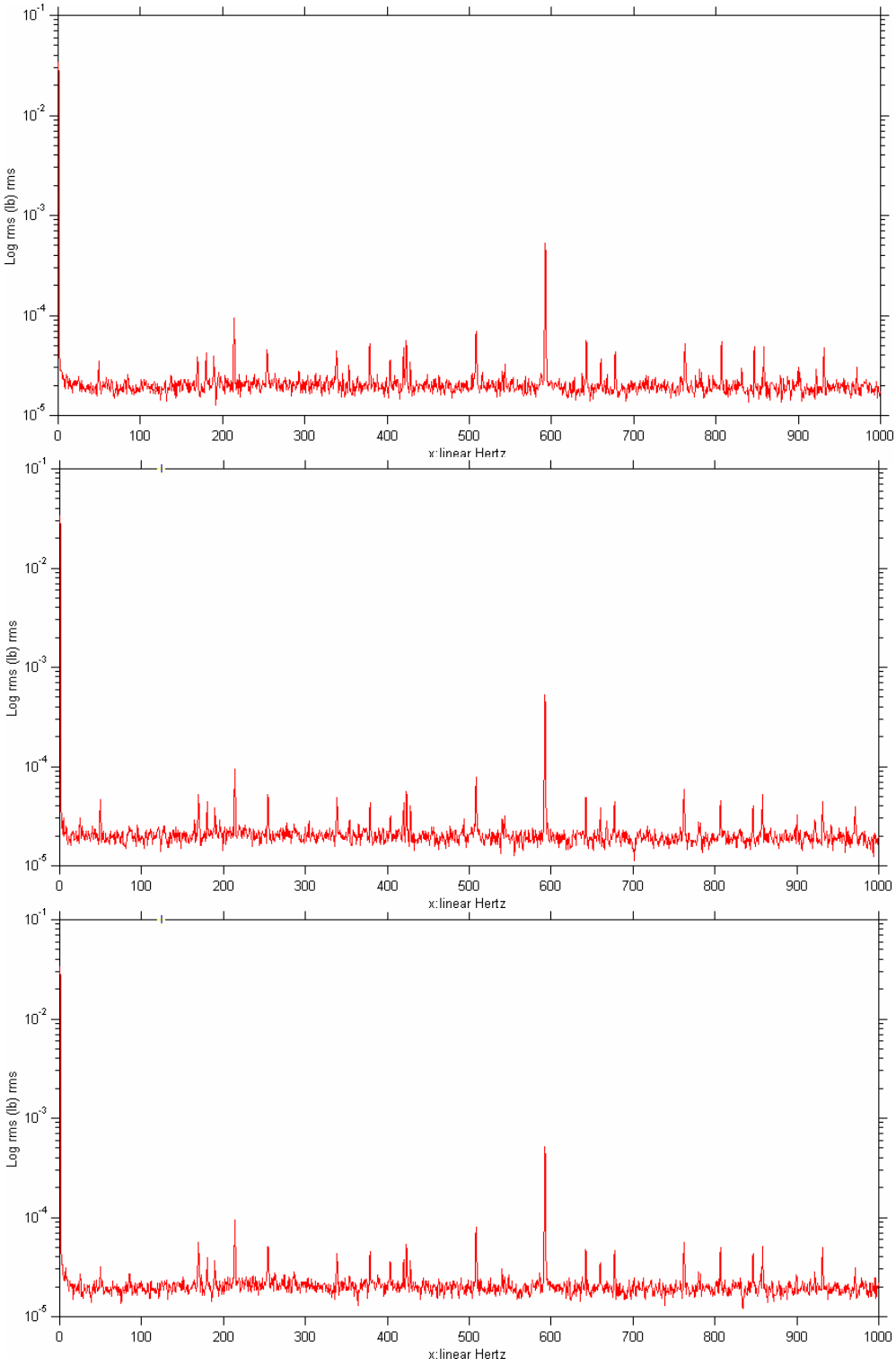

Figure 4.10: Frequency Spectrum Measured from the Palm of the Hand during Continuous Operation of a Reciprocating Saw over Three Trials

5.0 CONCLUSION & RECOMMENDATIONS

Previous studies utilizing this force measurement system determined that it was possible to measure a force applied to the handle of a vibratory hand tool, both static as well as dynamic, with frequencies up to 1600 Hz. Similarities were found between the dominant peaks of the acceleration and force spectrum over the bandwidth of the instrument amplifier. However, this analysis was limited to one tool and no data was presented regarding the repeatability of tests.

The study of multiple tool types, of varying operating mechanisms and occupational use were used in this study to broaden comparisons of the force and acceleration spectra in order to better understand the coupling interaction between a vibrating tool handle and its operator. In addition, transfer and coherence functions were calculated to better quantify this coupling interaction. The effects of mounting the force sensor on the palm versus the finger were also evaluated. Repeatability tests were also conducted.

The forces observed during the operation of the rotary tool types were much lower in magnitude than those observed for the impact type. Though similar, harmonic peaks were observed for the force frequency spectra which where not observed for the acceleration frequency spectra. The force magnitudes of the resonant spikes were most prominent for the grinder, which exhibited the lowest force magnitudes within its frequency spectrum. Contrary to the rotary type tools, the chipping hammer produced significantly higher magnitudes of force and acceleration throughout the frequency

bandwidth. For this tool, similarities were observed between data from each measurement system and harmonic peaks were not observed in the force data.

The harmonic peaks may be the result of insufficient coupling of the hand with the tool-handle. This would result in a smaller normal force acting on the sensor, and may allow the sensor to move with respect to the tool handle and the hand and this motion would dominate the signal. The decreased coupling force required to operate the grinder tool resulted in an increase in this harmonic response. Alternatively, the coupling force required to operate the chipping hammer exhibited a significant reduction in the magnitude of these spikes. The resonance may also be the result of the motion of the finger with respect to the handle. However, the resonant spikes were not observed when the sensor was mounted directly to the handle for either the finger or palm measurements on the saw handle. It is believed that the spikes are the result of resonance of the force sensor itself and can be reduced when measurements are made directly on the tool handle or when a sufficient coupling force is required for tool operation.

With consideration to the systems electronic characteristics, the output signal may be susceptible to secondary electronic effects such as interference from an electromagnetic noise source. Previous studies have shown that these effects could be minimized if the pre-amplifier was sufficiently shielded. Such shielding was designed in this study. However, as a result of a small magnitude applied force the output of the force sensor is very small and noise contributions may contribute more to the overall amplified signal. Hence, the effects of noise and interference may be more dominate when tools requiring a low magnitude coupling force are used.

Transfer and coherence functions provide a very useful way to look at the relationship between the force and acceleration data when interpreting the cause/effect relationship at the handle interface. Consistent, or linear, zones within an estimated transfer function may represent that a definitive causal relationship exists between input/output signals. Such relationships existed for the chipper hammer, drill, and die grinder at frequencies less than 200, 100, and 200 Hz, respectively. With respect to the corresponding coherence functions, the chipping hammer results were determined to have the highest confidence. The highest coherence was for the first dominant frequency at 50 Hz, and decreasing thereafter. The two rotary tools exhibited relatively low coherence throughout the 200 Hz bandwidth. This may reflect the low coupling forces at the handle interface. As a result of the impending vibration, insufficient coupling may result in a greater contribution of the tissue response to the frequency spectra as well as allowing resonance of the force sensor. These effects would contribute to a non-linear relationship between the acceleration measured on the tool and the force measured at the finger.

Finger and palm mounting of the force sensor produced similar frequency spectra. However, the magnitudes of force at the two different locations of the hand reveal significant results. The forces observed when mounting the sensor to the finger were lower in magnitude than when mounted on the palm. This effect can be attributed to the push force (summation of the grip and feed forces) measured at the palm. Furthermore, the respective transfer and coherence functions for the two mounting locations reveal that the mechanical attributes of soft tissue are more prominent when the operator-handle force is measured at the finger. This result can be attributed to the dynamic response of

soft tissue and resonance of the finger itself in addition to the finger's geometry. Force is applied to the handle by the finger primarily through the distal and proximal ends of each phalange. Thus tissue between these simply-supported joints does not exert the greatest magnitude force to the handle and primarily respond to the vibration by dampening the force.

The force instrumentation system was shown to produce accurate and repeatable results over the tested bandwidth. The frequency response of the sensor was reliable in showing the dynamics of the hand-handle coupling. Static tests of the sensor showed on average a 25% error before and after tool testing. This error resulted from a reduction of the output voltage of the sensor. The reduction may be attributed to distribution of the sensor's ink following its exposure to vibration. Performing a static test in order to determine how variations in the ink distribution change with respect to time affect the sensor's resistance to force may validate this statement. Other errors of the force sensor may be the result of exposure to shear forces during tool operation. This can be tested by applying a static load to the sensor which has both normal and tangential components in order to determine the variation of the sensor's output voltage as a function of applied shear force.

In conclusion, large accelerations are produced by vibratory tools. This energy is transferred through the handle of the tool to its operator. The dominant forces exerted on the operator's hands most likely occur at the same dominant frequencies as the acceleration modes of the tool. Some variations between force and acceleration do occur as the result of acceleration independent factors. Such factors include, but are not limited to, the re-gripping of the tool and tool impacts. Tool re-gripping reveals the tonal

response of the muscles of the hand to the impending vibration. Tool impacts are frequency independent (0 Hz) responses caused by impacts of the tool with its operating surface. The forces produced by the tool are exerted to the hand via the tool's handle and the energy is dissipated. The dissipation of energy by the hand is mostly contributed by the excellent dampening properties of soft tissue as well as resonance of the hand. The impending vibration causes irreversible damage to nerves and blood vessels thus causing the soft tissue disease, HAVS. Hence, it is of the utmost importance to protect the operator's hands when utilizing vibrating hand-held tools of any type. Additionally, well engineered tools exhibiting anti-vibration technology and implementing dynamic dampening elements should be produced to further decrease the user's risks of permanent, debilitating injury, as the result of the occupational hazards of hand-held vibrating equipment.

Further studies of the coupling response between an operator and vibrating tool should investigate the effectiveness of gloves in the reduction of hand transmitted vibration. A force measurement system and procedure similar to the one used in this study may evaluate the mechanical performance of the anti-vibration materials used in professional gloves. It is suggested that data measurements be taken on a bony surface of the hand on the palm side of the handle of a highly percussive tool (i.e. chipping hammer) to assure that a sufficient coupling force is present at the handle. This will minimize resonance of the sensor and further reduce the non-linear mechanical contribution of soft tissue. In effect, the study results may primarily be indicative of the transmissibility of the glove material when the force is measured both between the handle-glove and the glove-user. In addition, it may be of interest to incorporate larger populations to explore

other factors such as the variations in coupling effects for users with different hand sizes and hand geometries, grip strengths, and experience with tool use. It is also suggested that further studies of the force instrumentation system incorporate a force-time analysis as well as quantification of the effects of shear forces on the force sensor.

REFERENCES

(1) Ahn, J. I. (2000). Design and Testing of Vibratory Force Measurement System for Hand-Arm Vibration Applications. Mechanical, Aerospace & Engineering Science. Knoxville, University of Tennessee: 62.

(2) Bovenzi, M., M. J. Griffin, et al. (1995). "Vascular Responses to Acute Vibration in the Fingers of Normal Subjects." Central European Journal of Public Health(3): 15-8.

(3) Bovenzi, M., C. J. Lindsell, et al. (2001). "Response of Finger Circulation to Energy Equivalent Combinations of Magnitude and Duration of Vibration." Occupational and Environmental Medicine **58**(6): 185-93.

(4) Dong, R., S. Rakheja, et al. (2001). "Hand-transmitted vibration and biodynamic response of the human hand-arm: a critical review." Critical Reviews in Biomedical Engineering **29**(6): 393-439.

(5) Dong, R., A. Schopper, et al. (2004). "Vibration energy absorption (VEA) in human fingers-hand-arm system." Medical Engineering and Physics **26**(8): 483-92.

(6) Feutry, D., P. Lemerle, et al. (2004). Design of a New Instrumented Glove for the Measurement of the Contact Pressure Distribution at the Hand/Handle Interface. 10th International Conference on Hand-Arm Vibration, Las Vegas, Nevada.

(7) Futatsuka, M., T. Miyakita, et al. (1996). "An Experimental Study on Changes on Finger Blood Pressure During Chain-Saw Operation." Industrial Health **34**: 93-100.

(8) Griffin, M.J. (1996). Handbook of Human Vibration. Harcourt Brace & Company, Publishers, New York.

(9) Jetzer, T., P. Haydon, et al. (2003). "Effective intervention with ergonomics, antivibration gloves, and medical surveillance to minimize hand-arm vibration hazards in the workplace." Journal of Occupational and Environmental Medicine **45**(15): 1312-7.

(10) NIOSH. (1983). “Current Intelligence Bulletin 38: Vibration Syndrome.”

(11) Pelmear, P. L., W. Taylor, et al. (1992). Hand-arm Vibration: A Comprehensive Guide for Occupational Health Professionals. New York, Van Nostrand.

(12) Schenk, T. (1995). "Statistical Analysis of Vibration-Induced Bone and Joint Damages." Central European Journal of Public Health **3**: 113-7.

(13) Wasserman, Donald E. (1987). Human Aspects of Occupational Vibration. Elsevier, New York.

(14) Wasserman, D. E., J. F. Wasserman, J. I. Ahn. (2001). Instrumentation for Measuring Coupling Forces of Hand-Held Tools. Sound and Vibration. 35: 22-25.

(15) Wasserman, D. E. and J. F. Wasserman (2004). The Paradox of Vibration Control and Ergonomics. Compliance Magazine. **11**: 15.

(16) Wieslander, G., D. Norback, et al. (1989). "Carpal Tunnel Syndrome (CTS) and Exposure to Vibration, Repetitive Wrist Movements, and Heavy Manual Work: A Case-Referent Study." British Journal of Industrial Medicine **46**(1): 43-7.

APPENDIX A

ADDITIONAL ACCELERATION FREQUENCY SPECTRUMS

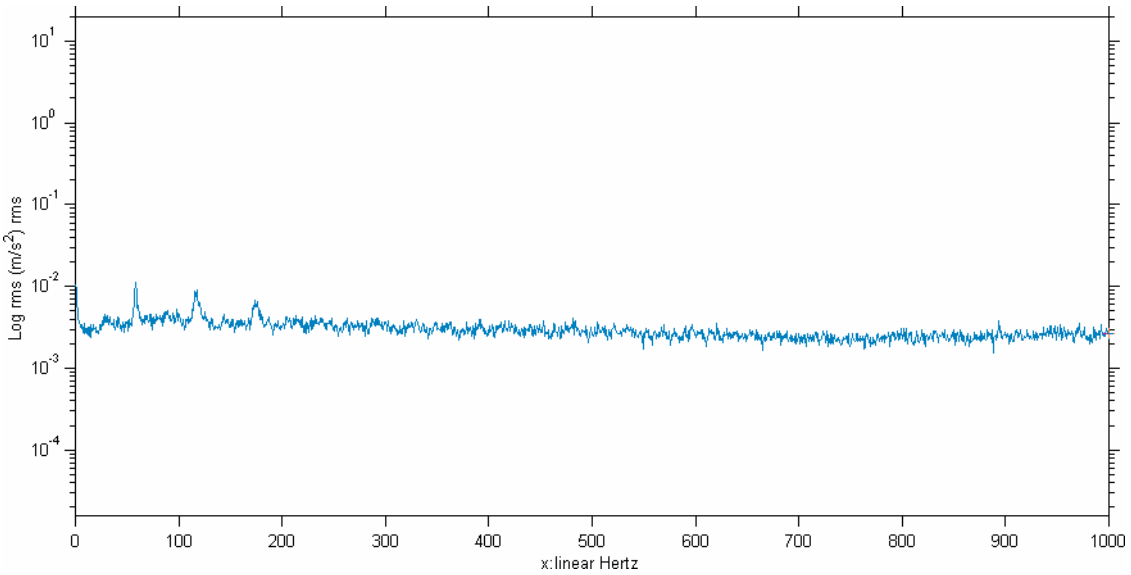

Figure A.1: X-Direction Acceleration Frequency Spectrum for Continuous Operation of Impact Hammer with Chisel Tip

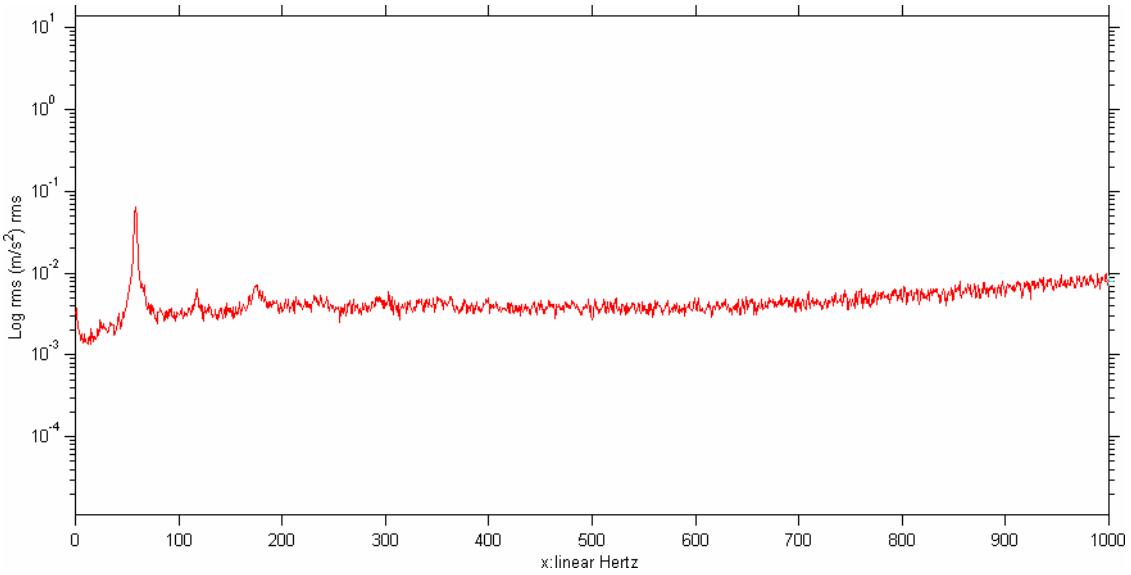

Figure A.2: Y-Direction Acceleration Frequency Spectrum for Continuous Operation of Impact Hammer with Chisel Tip

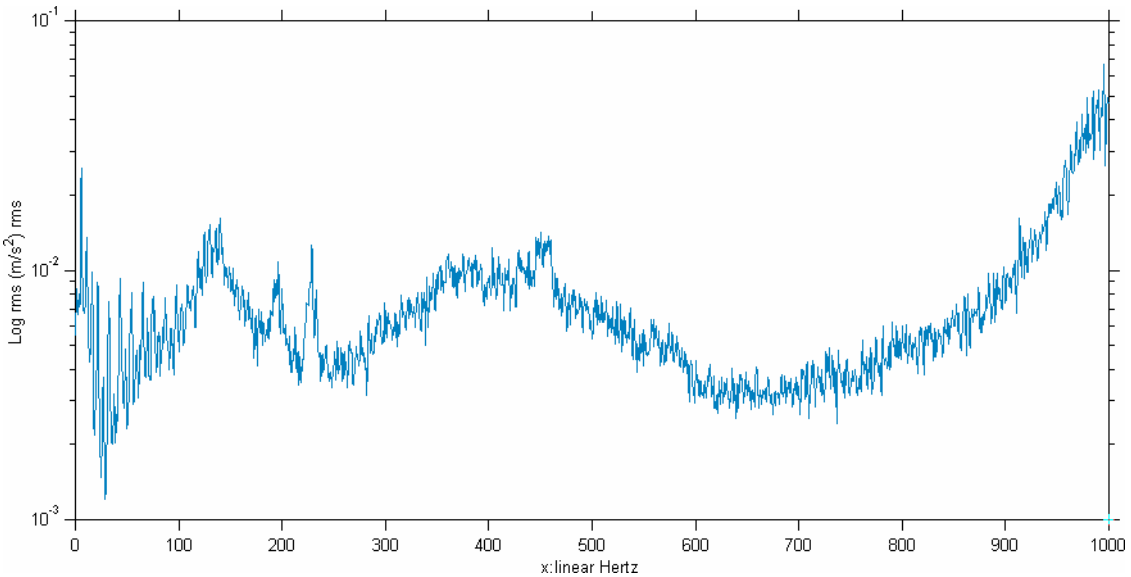

Figure A.3: X-Direction Acceleration Frequency Spectrum for Continuous Operation of Drill

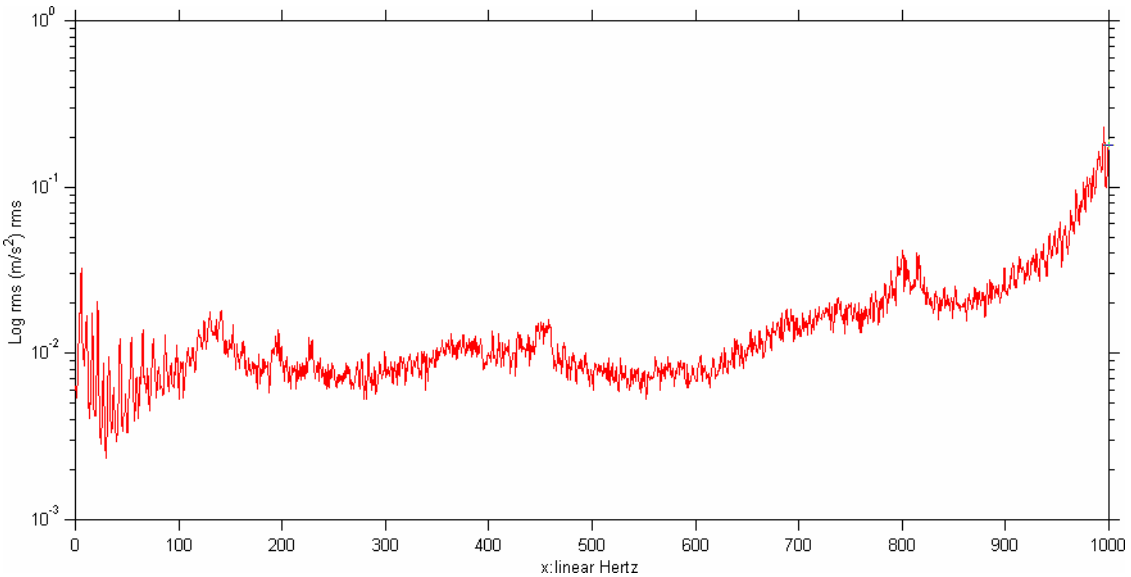

Figure A.4: Y-Direction Acceleration Frequency Spectrum for Continuous Operation of Drill

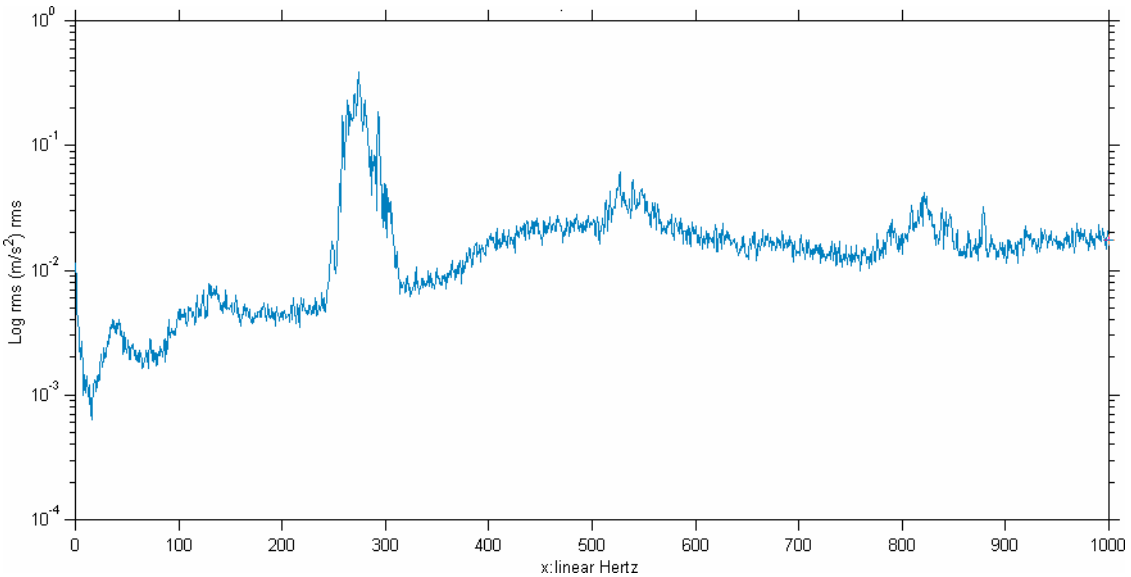

Figure A.5: X-Direction Acceleration Frequency Spectrum for Continuous Operation of Die Grinder

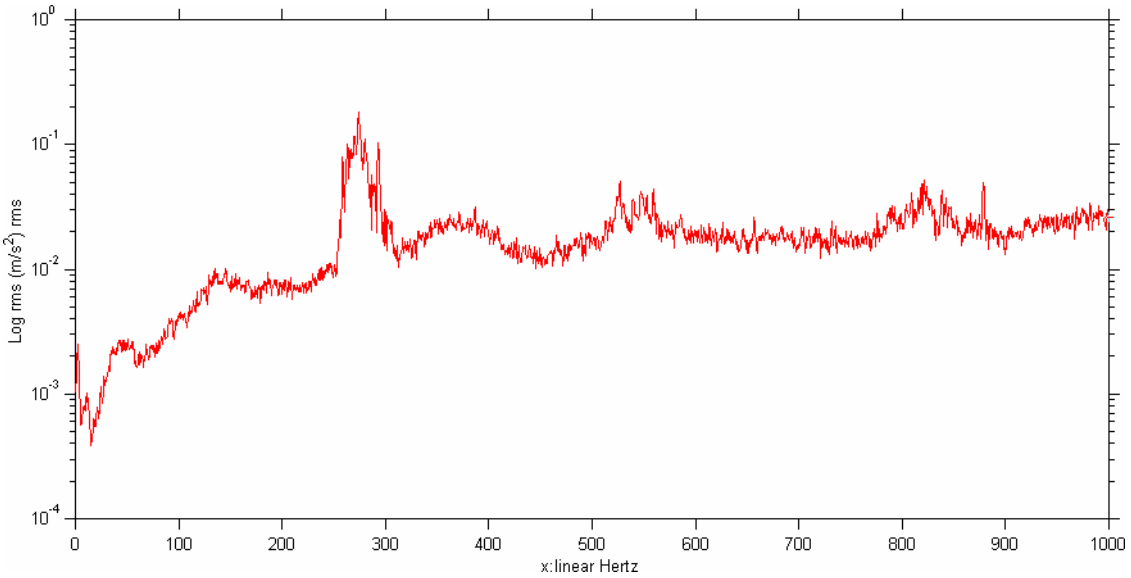

Figure A.6: Y-Direction Acceleration Frequency Spectrum for Continuous Operation of Die Grinder

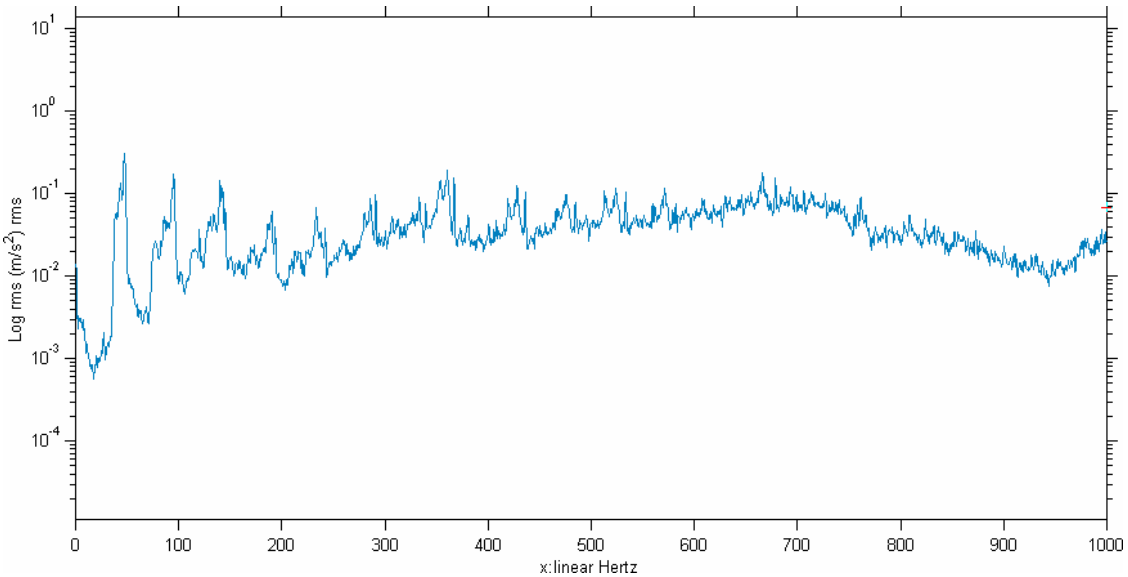

Figure A.7: X-Direction Acceleration Frequency Spectrum for Continuous Operation of Reciprocating Saw

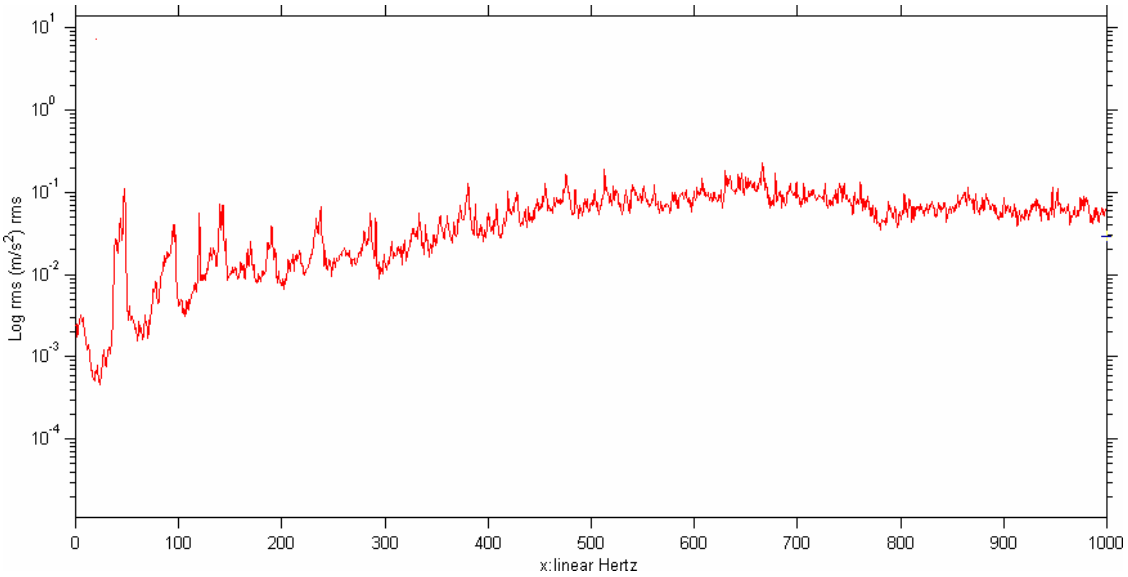

Figure A.8: Y-Direction Acceleration Frequency Spectrum for Continuous Operation of Reciprocating Saw

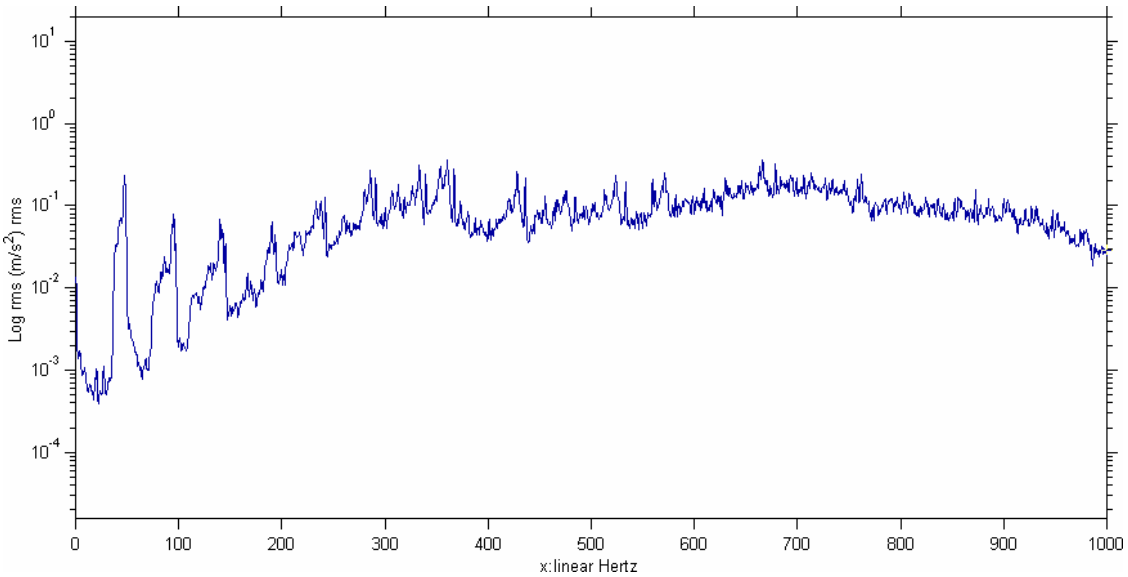

Figure A.9: Z-Direction Acceleration Frequency Spectrum for Continuous Operation of Reciprocating Saw

APPENDIX B

FREQUENCY SPECTRUM AND TRANSFER FUNCTION FROM IMPACT HAMMER WITH SPLITTER TIP

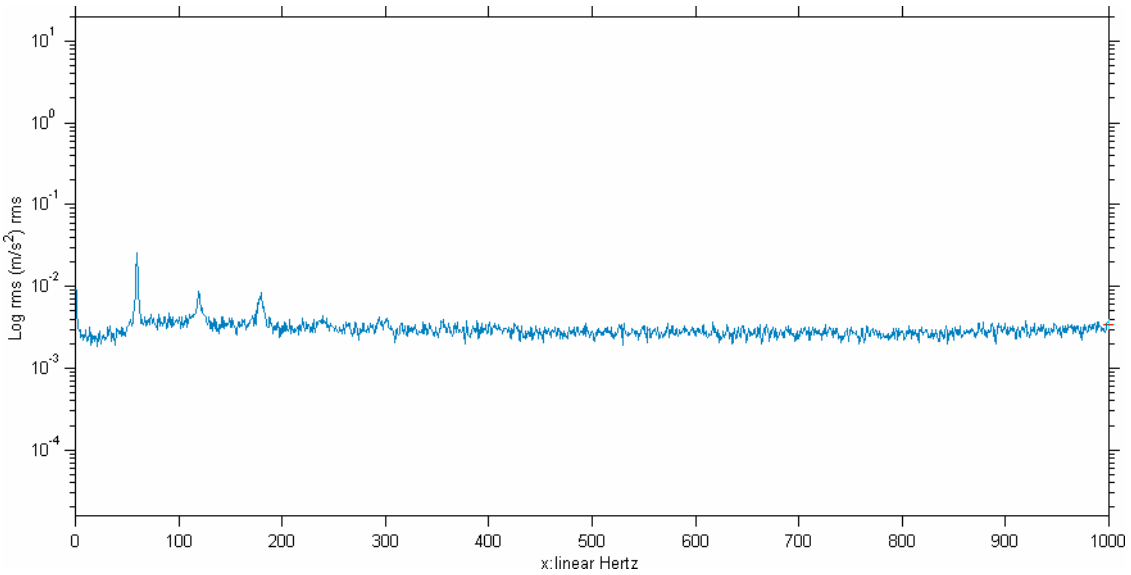

Figure B.1: X-Direction Acceleration Frequency Spectrum

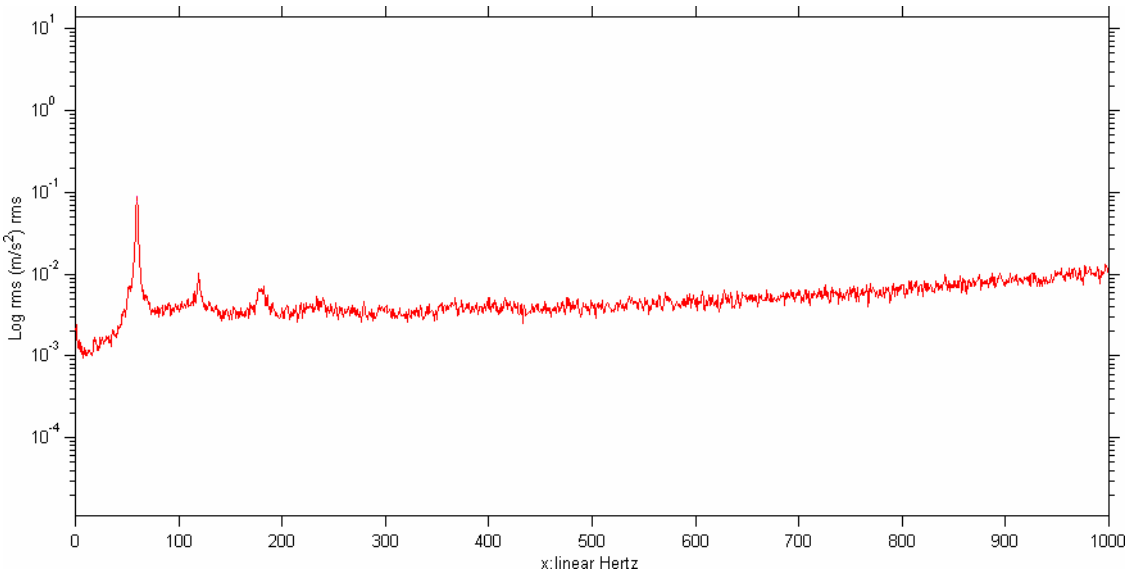

Figure B.2: Y-Direction Acceleration Frequency Spectrum

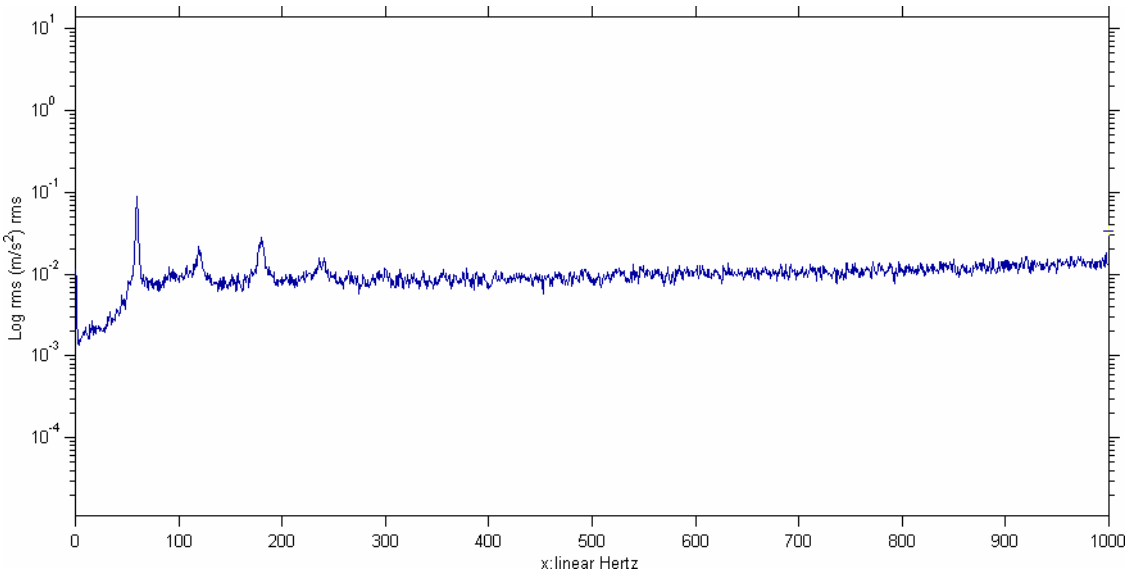

Figure B.3: Z-Direction Acceleration Frequency Spectrum

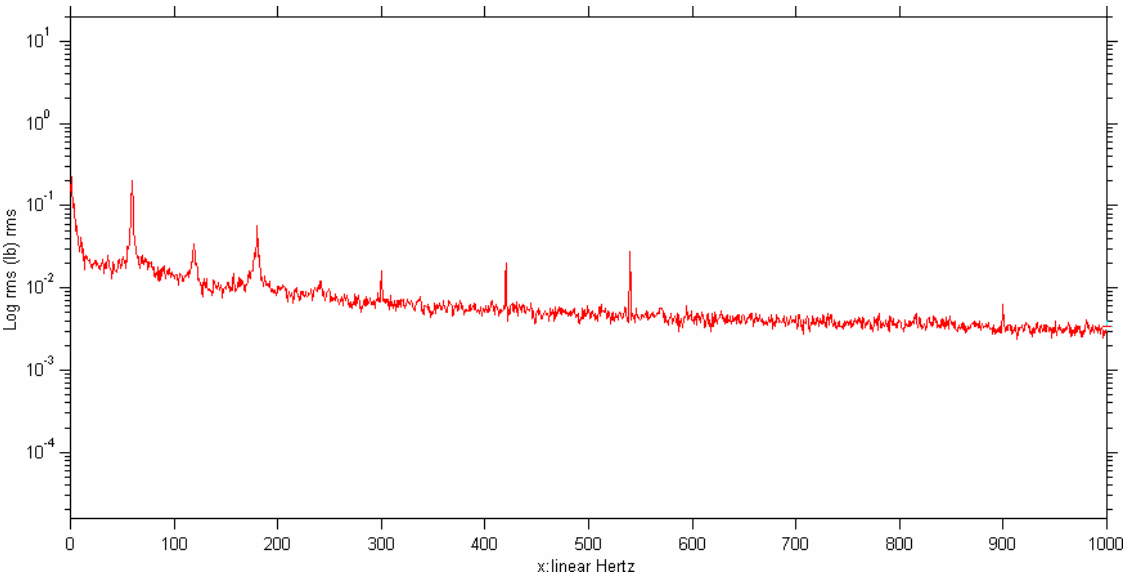

Figure B.4: Finger Force Frequency Spectrum

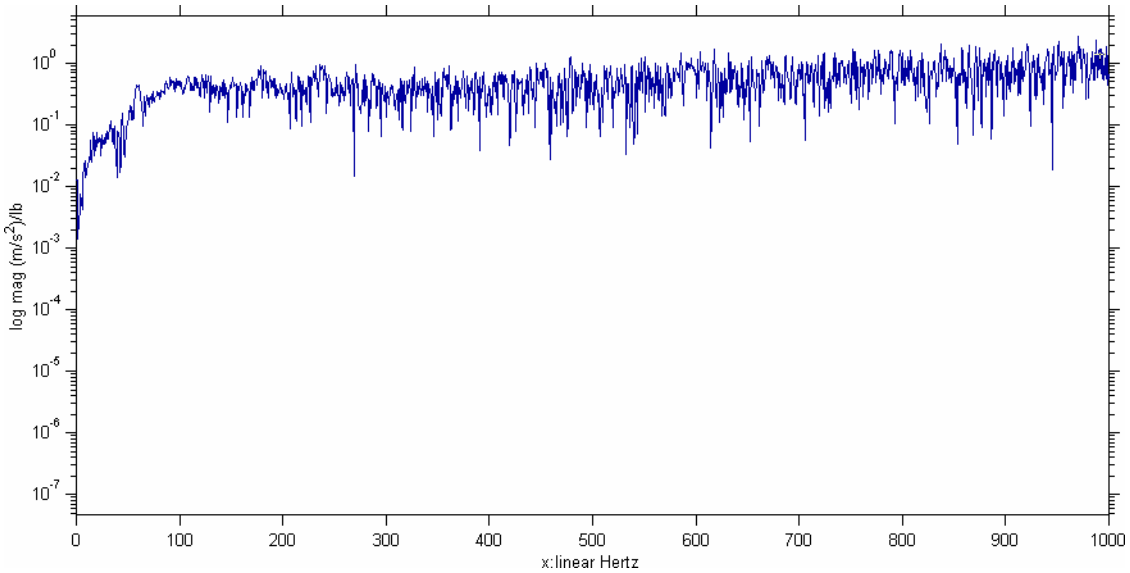

Figure B.5: Transfer Function for Acceleration-Force

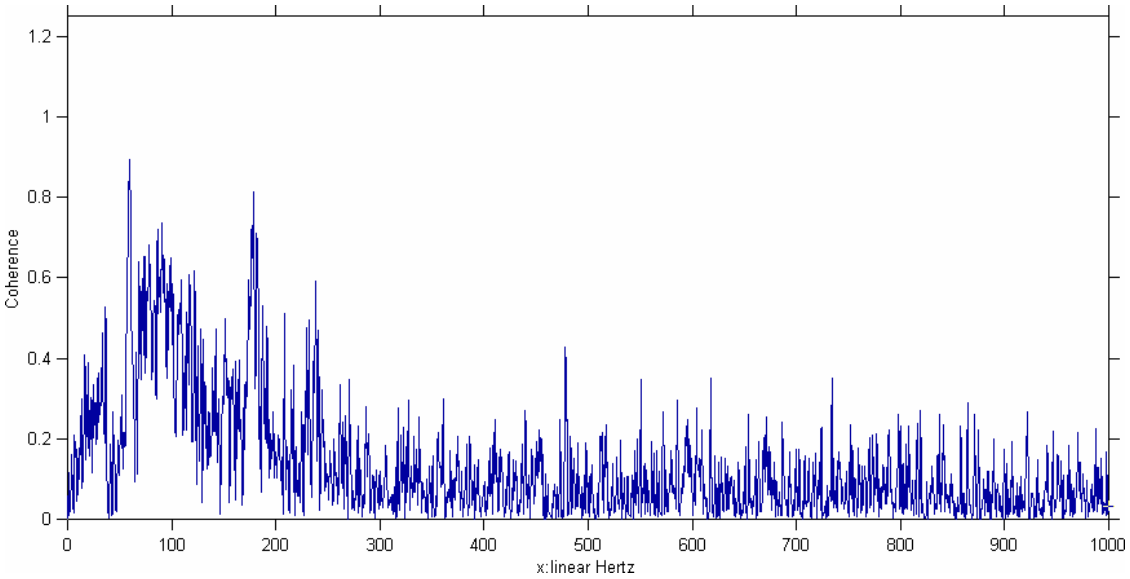

Figure B.6: Coherence Plot for Acceleration-Force

APPENDIX C

ACCELERATION FREQUENCY SPECTRA FROM REPEATABILITY TESTS

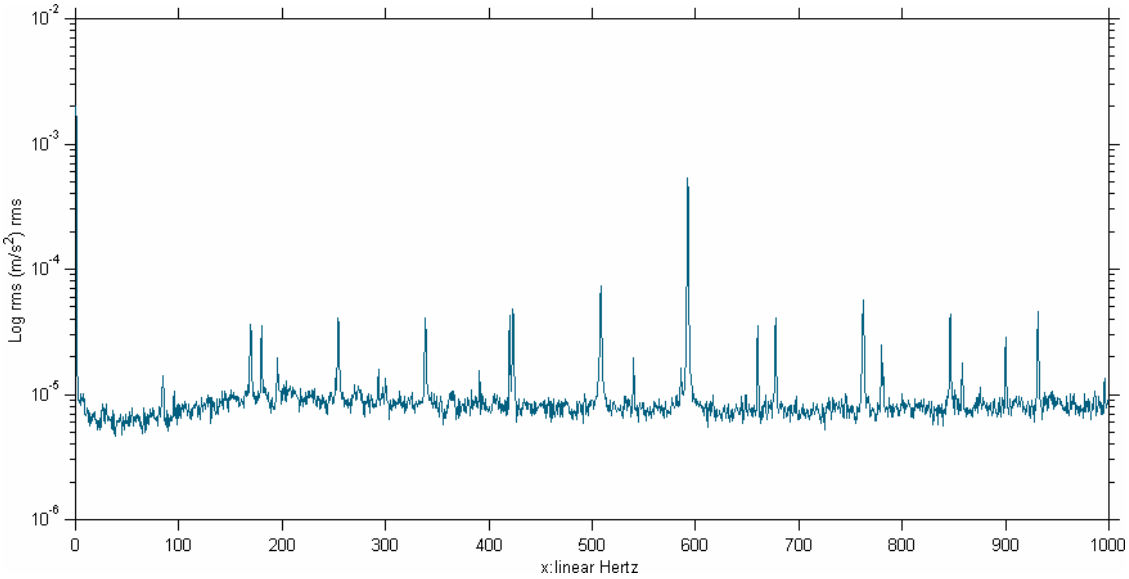

Figure C.1: X-Direction Acceleration Frequency Spectrum for Trial One

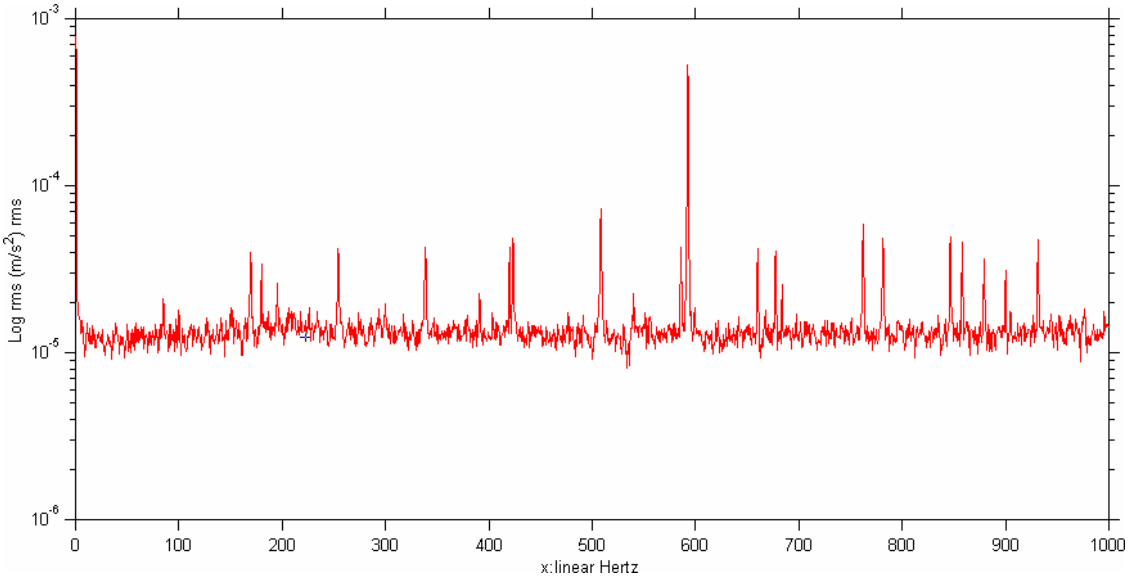

Figure C.2: Y-Direction Acceleration Frequency Spectrum for Trial One

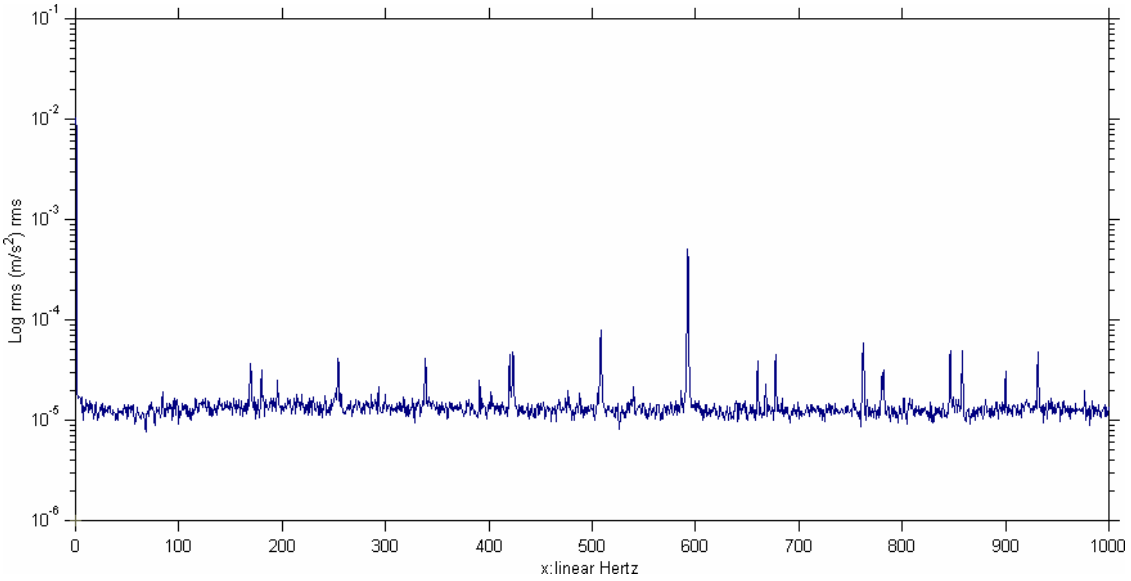

Figure C.3: Z-Direction Acceleration Frequency Spectrum for Trial One

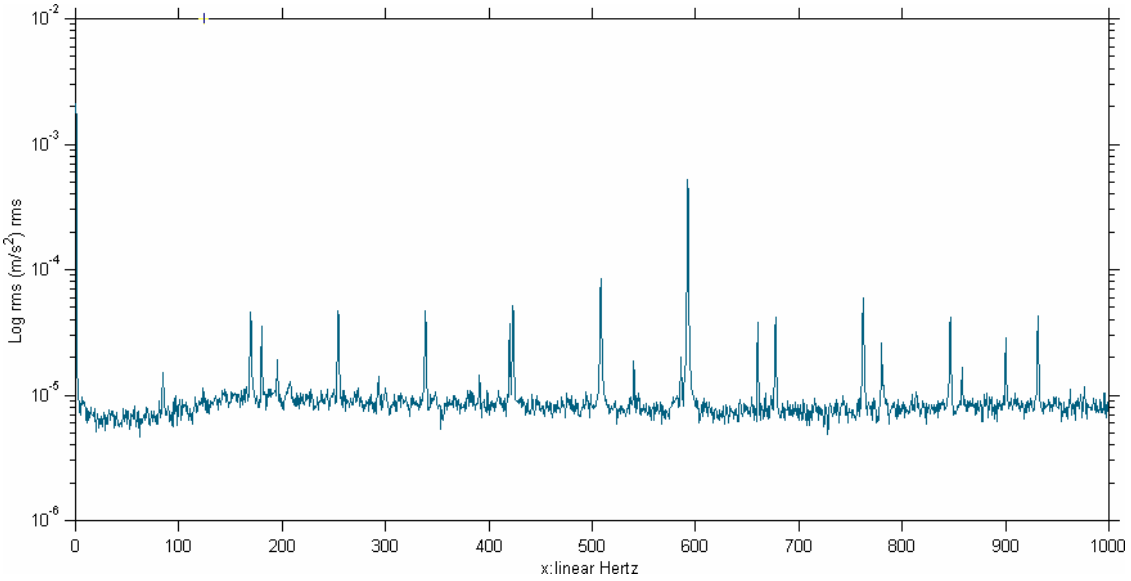

Figure C.4: X-Direction Acceleration Frequency Spectrum for Trial Two

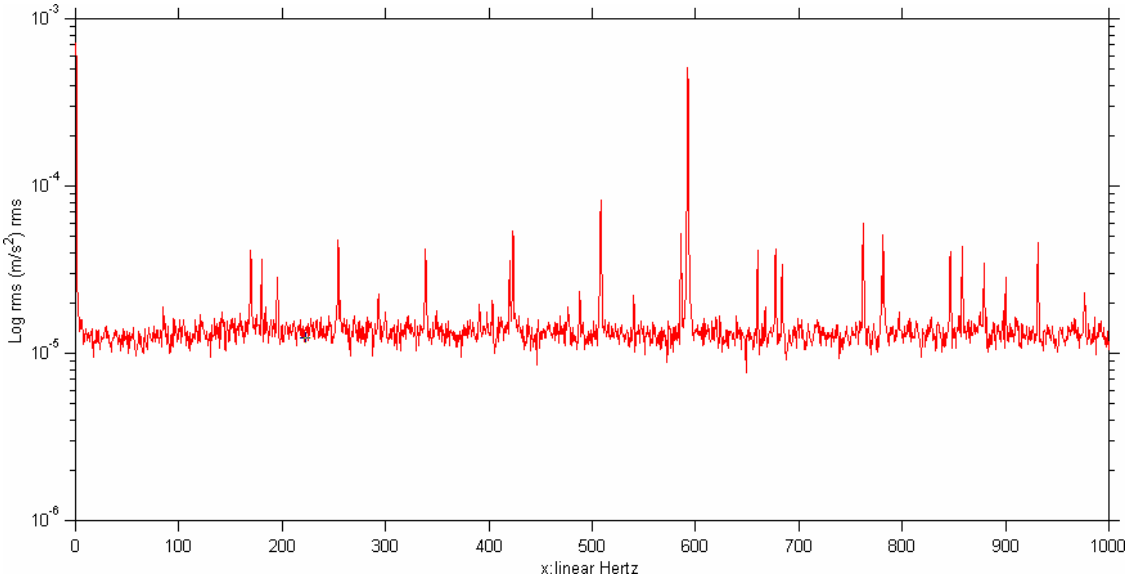

Figure C.5: Y-Direction Acceleration Frequency Spectrum for Trial Two

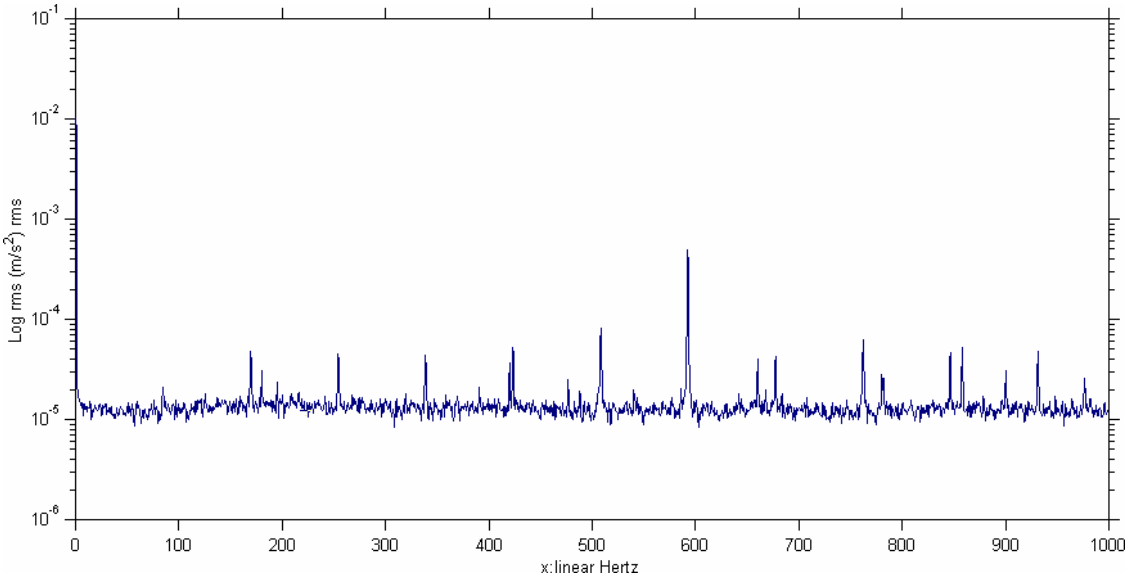

Figure C.6: Z-Direction Acceleration Frequency Spectrum for Trial Two

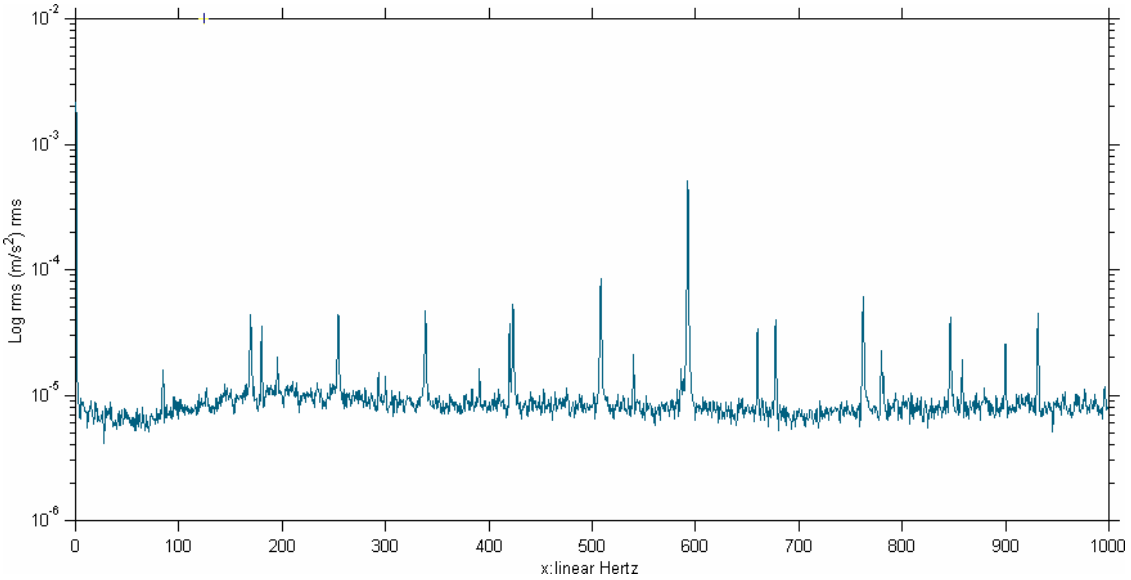

Figure C.7: X-Direction Acceleration Frequency Spectrum for Trial Three

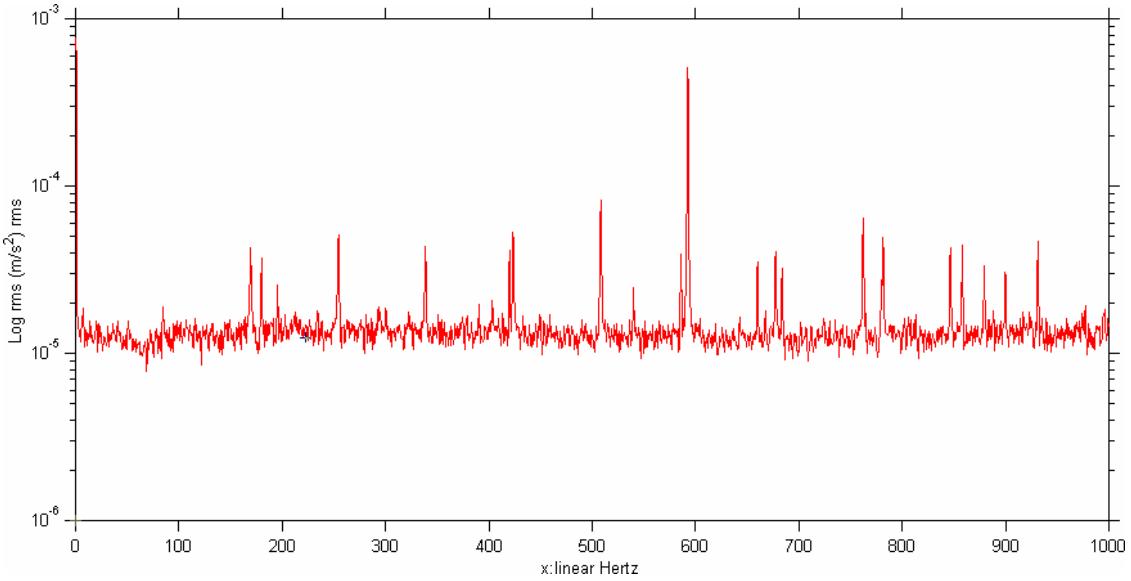

Figure C.8: Y-Direction Acceleration Frequency Spectrum for Trial Three

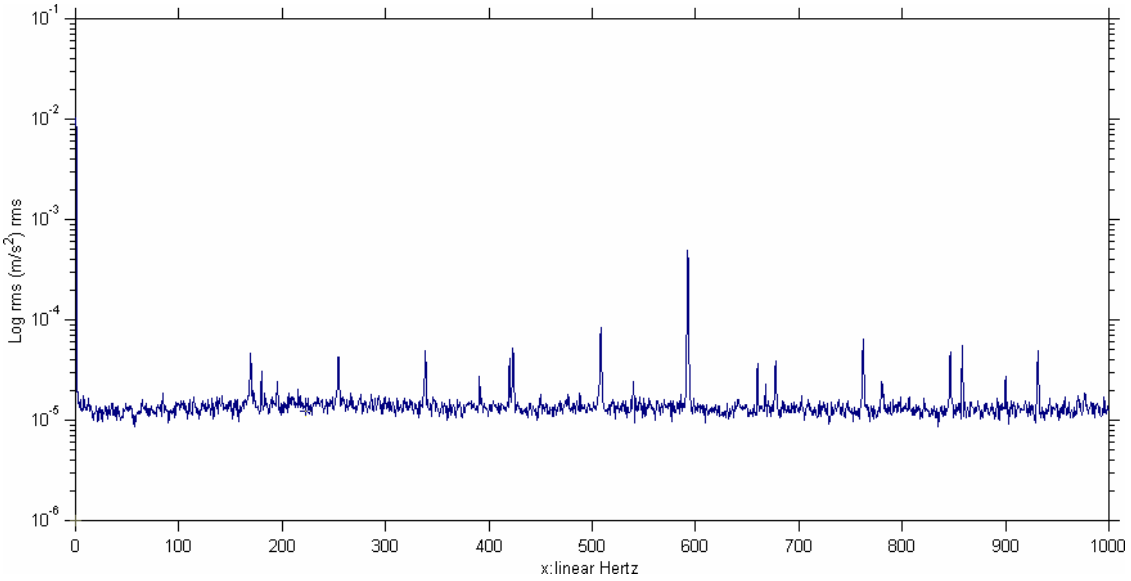

Figure C.9: Z-Direction Acceleration Frequency Spectrum for Trial Three

APPENDIX D

3RD OCTAVE PLOTS FROM ENGINEERING STANDARD ANALYSIS

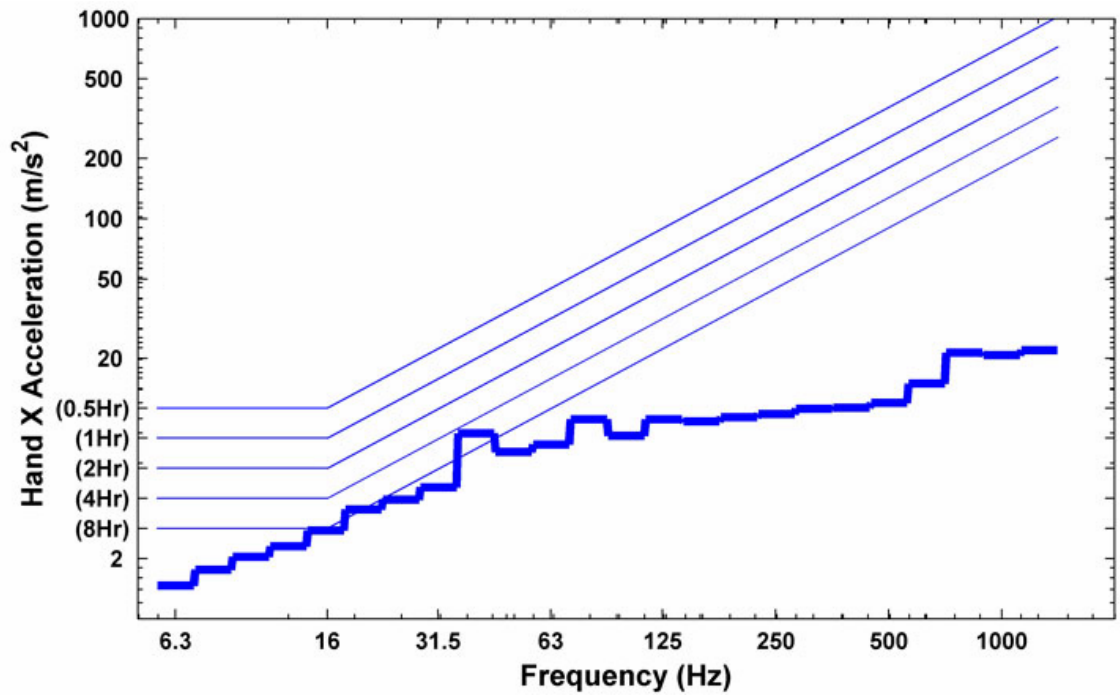

Figure D.1: 3rd Octave Analysis for X-Direction Impact Hammer (Chisel Tip)

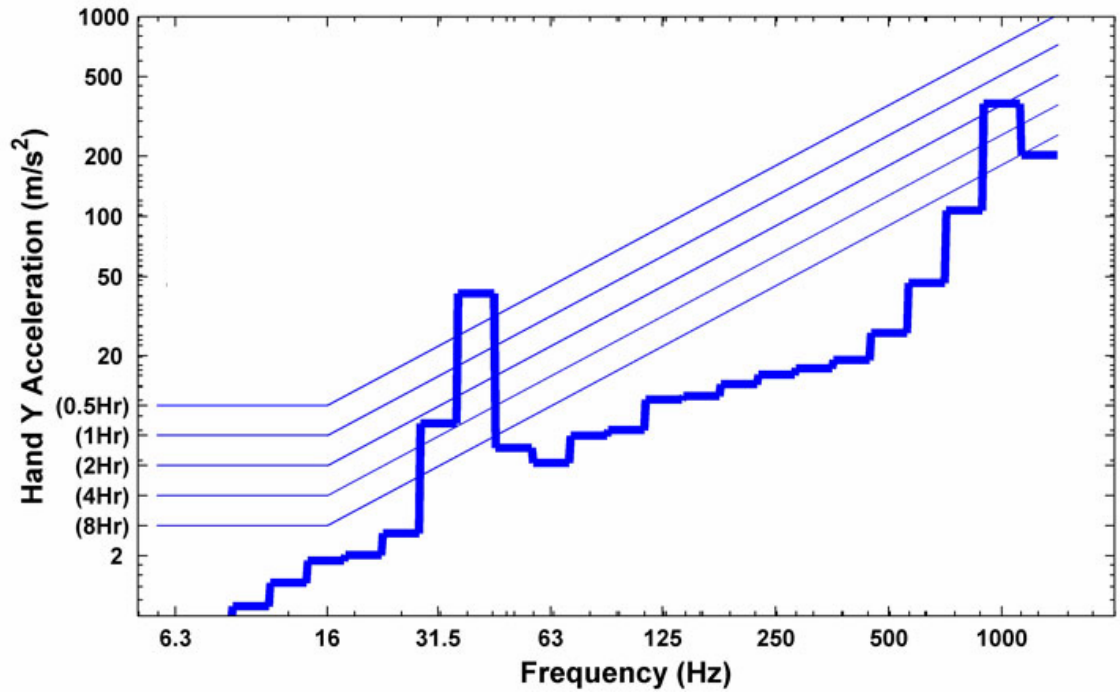

Figure D.2: 3rd Octave Analysis for Y-Direction Impact Hammer (Chisel Tip)

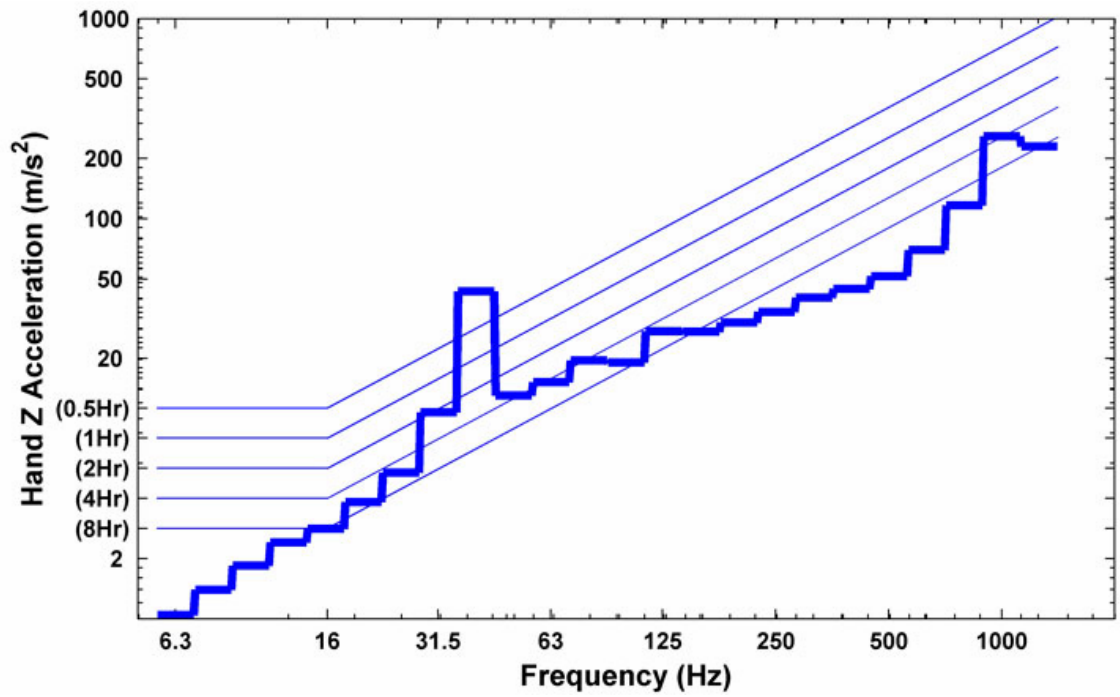

Figure D.3: 3rd Octave Analysis for Z-Direction Impact Hammer (Chisel Tip)

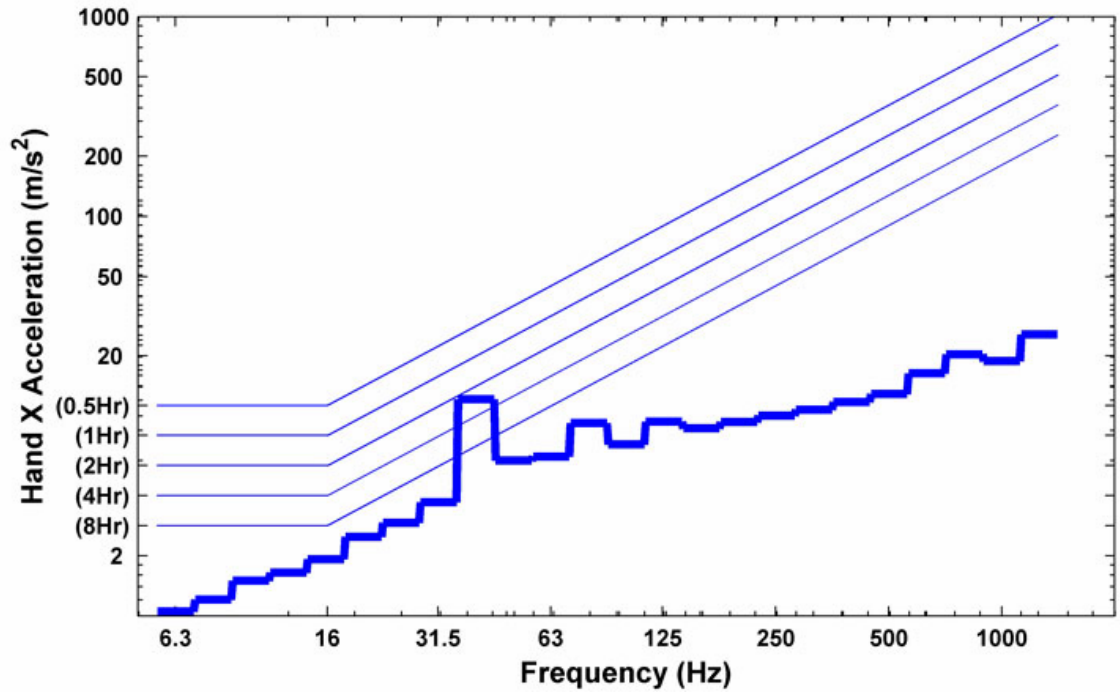

Figure D.4: 3rd Octave Analysis for X-Direction Impact Hammer (Splitter Tip)

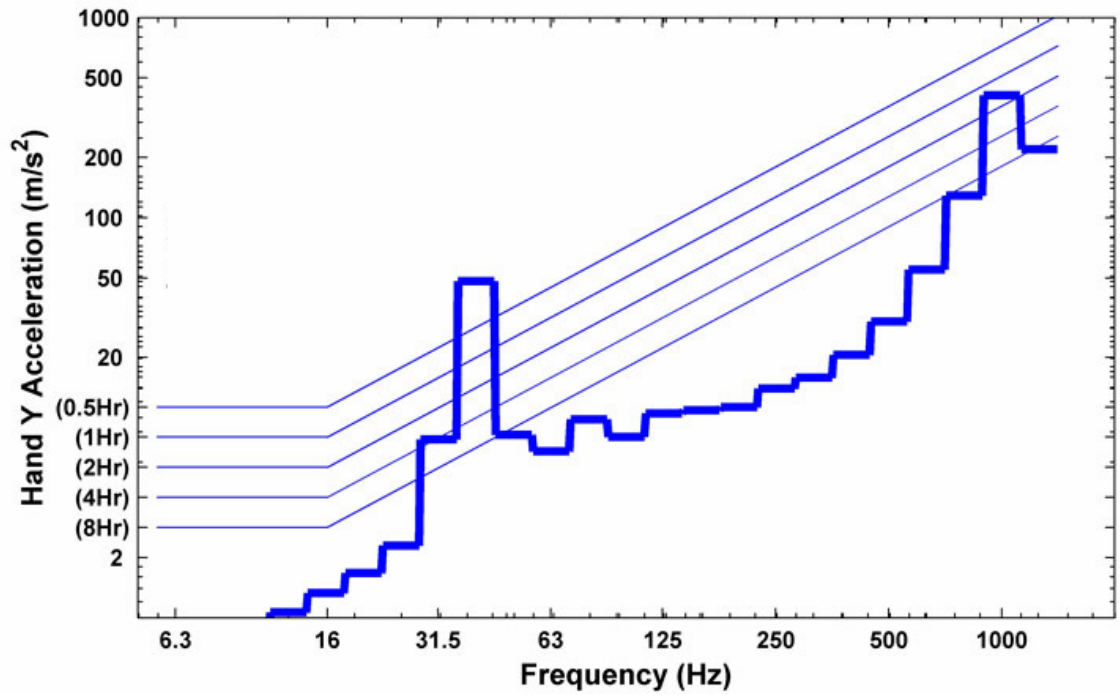

Figure D.5: 3rd Octave Analysis for Y-Direction Impact Hammer (Splitter Tip)

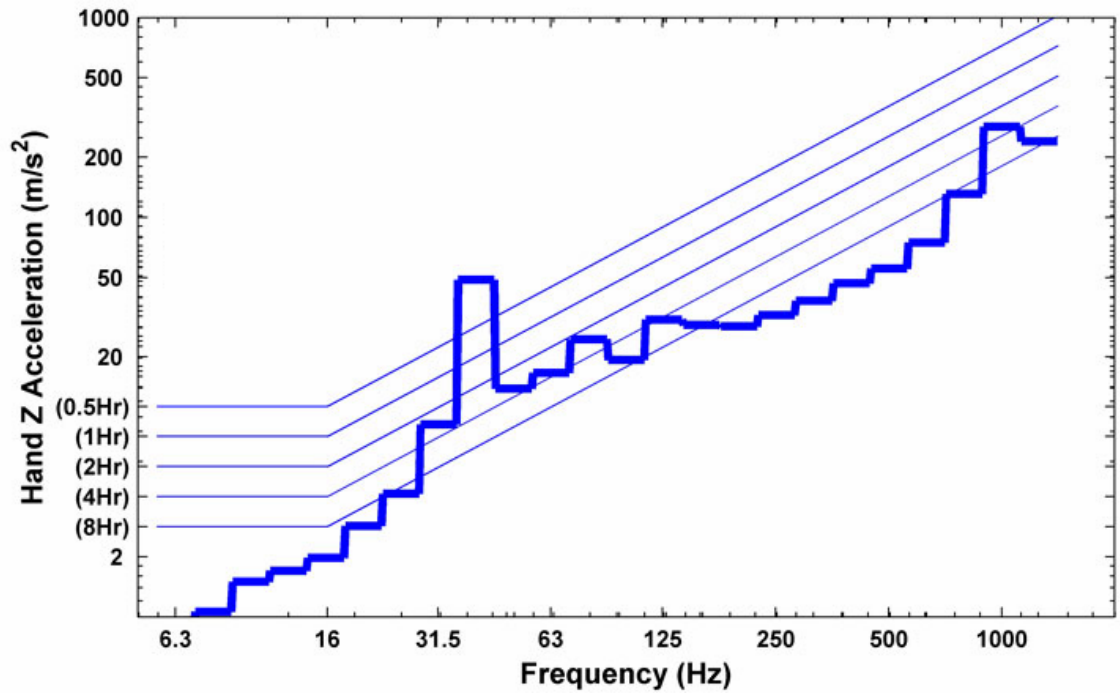

Figure D.6: 3rd Octave Analysis for Z-Direction Impact Hammer (Splitter Tip)

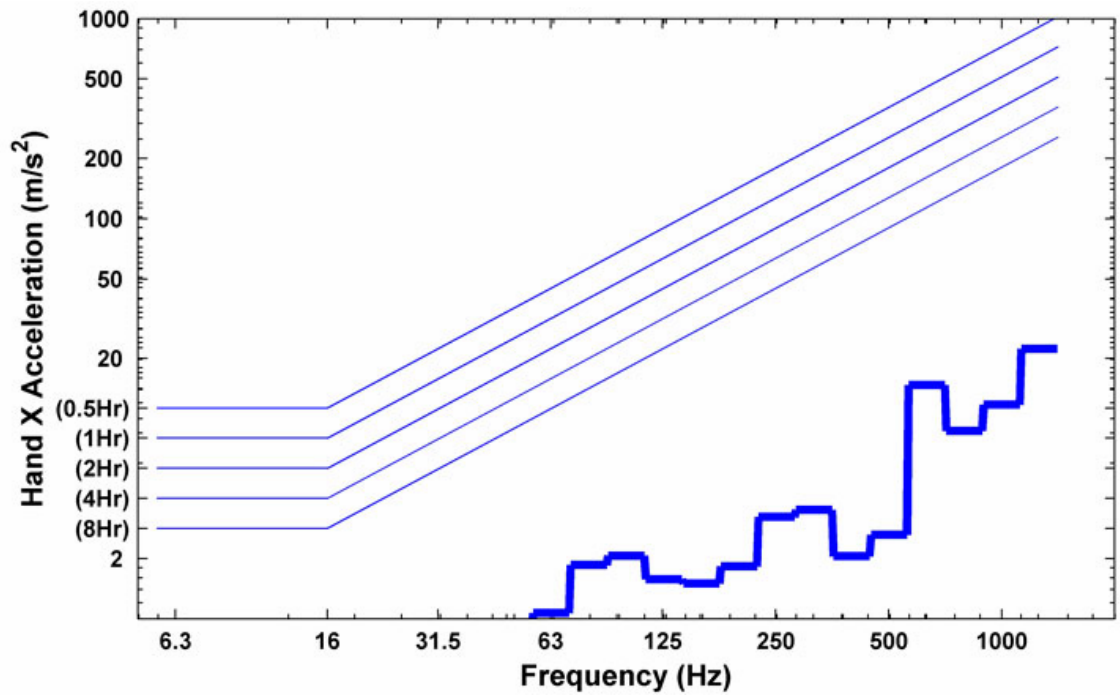

Figure D.7: 3rd Octave Analysis for X-Direction Drill

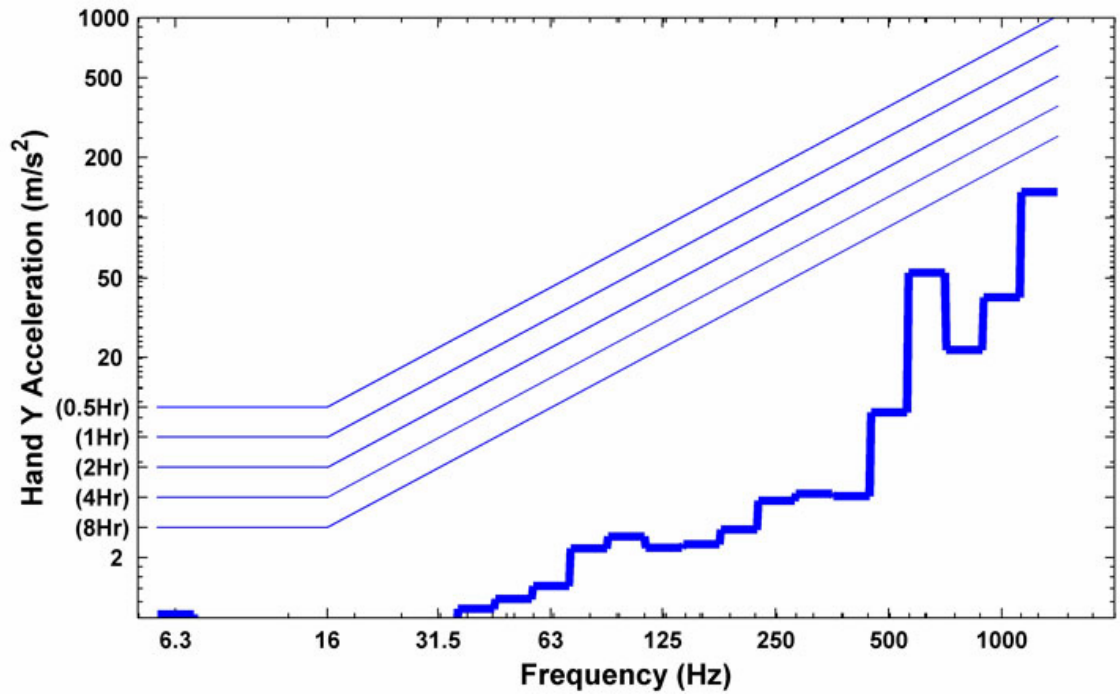

Figure D.8: 3rd Octave Analysis for Y-Direction Drill

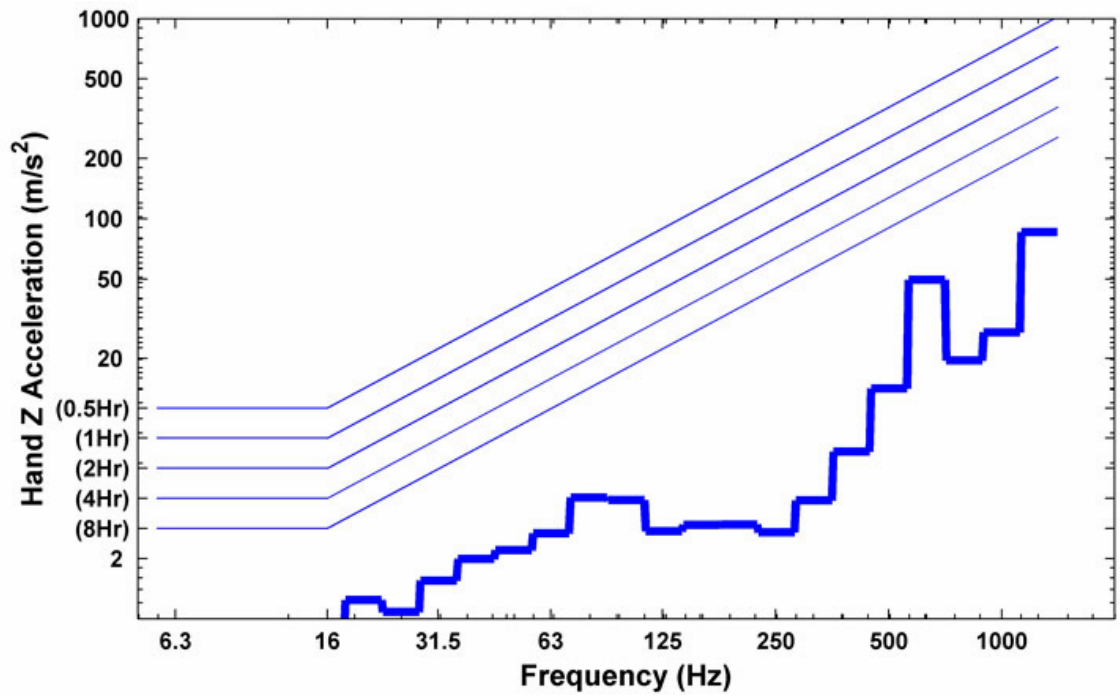

Figure D.9: 3rd Octave Analysis for Z-Direction Drill

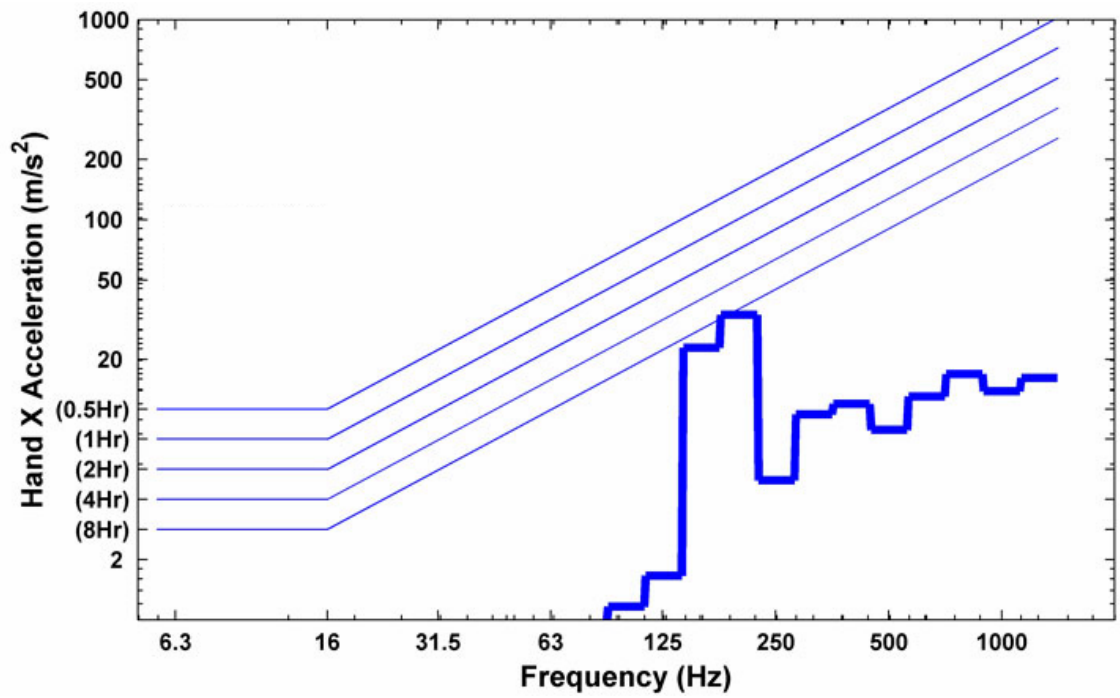

Figure D.10: 3rd Octave Analysis for X-Direction Die Grinder

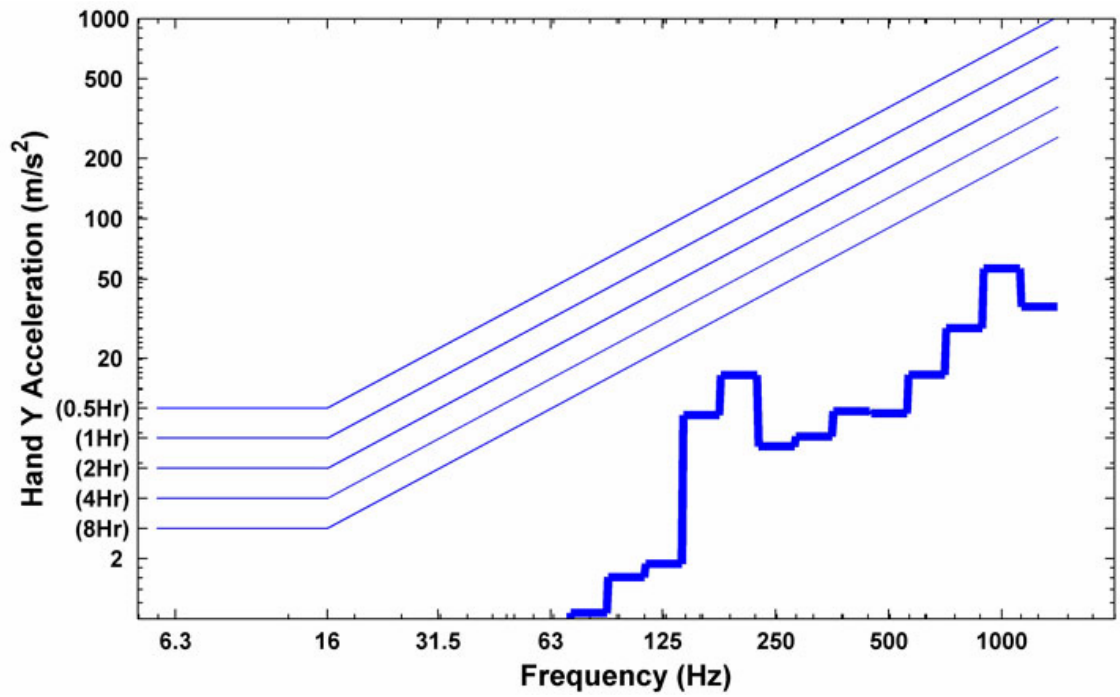

Figure D.11: 3rd Octave Analysis for Y-Direction Die Grinder

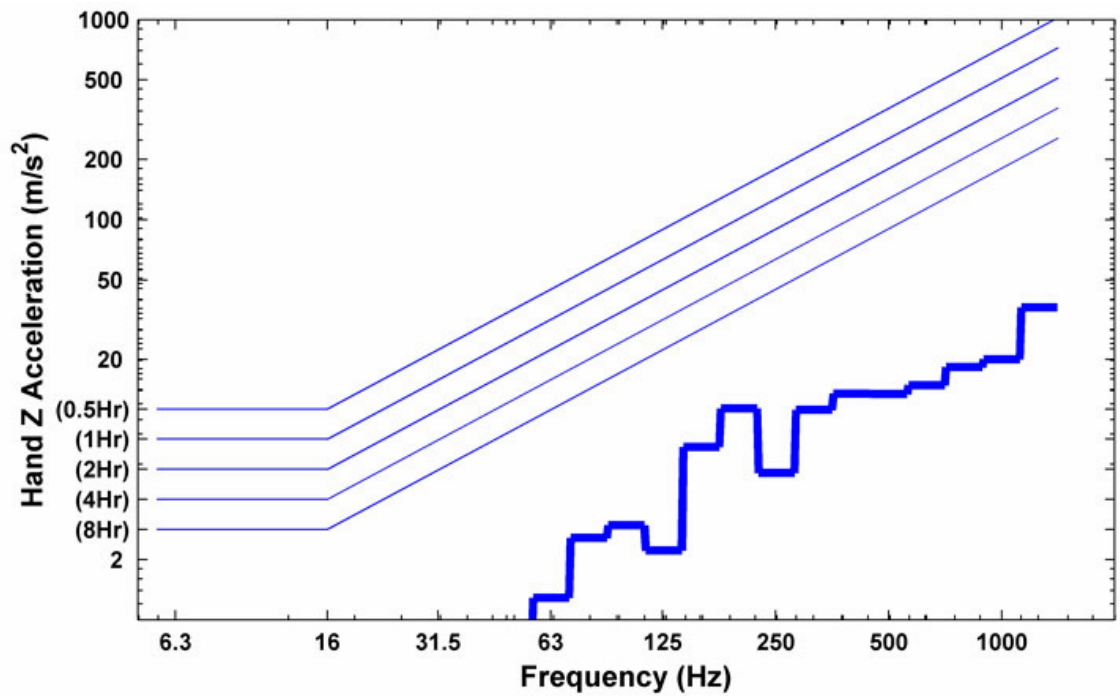

Figure D.12: 3rd Octave Analysis for Z-Direction Die Grinder

VITA

Douglas Alan Logsdon was born on March 21, 1978, in Royal Oak, Michigan. In the summer of 1992, he and his family moved to Knoxville, TN, where he was enrolled at Farragut High School. During his senior year, he was first introduced to the Biomedical Engineering field when he took a class presenting the combination of Electrical Engineering and Human Physiology. After graduating from Farragut High School in 1996, he then enrolled at the University of Tennessee, Knoxville, and studied Engineering Science with an emphasis in Biomedical Engineering. During his undergraduate studies, he conducted experiments in both Materials Science as well as Biomedical Engineering labratories. His academic awards included the Raymon Shobe Scholarship, Outstanding Senior of the Year 2000, and inductance into the Tau Beta Pi National Engineering Honor Society. He graduated Summa Cum Laude in spring 2000. Continuing towards a Master's Degree, he re-enrolled at the University. While studying towards Master's, he worked on a team of engineers collecting and processing data to be used in lawsuits regarding hand-arm and whole-body vibration. He also instructed dynamic data acquisition and processing using specialized software for an upper level engineering course. In his last few years at the University, he developed interactive learning supplements using dynamic multimedia and web design to be used as an instructional tool to teach basic engineering principles to freshman and sophomore engineers. He graduated from the University of Tennessee, Knoxville, with a Master's in Engineering Science in May 2005.